Injection of Water above Gas for Improved Sweep in Gas EOR: Non-uniform Injection and Sweep

Adhitomo Sulistyo

TU Delft

Title	:	Injection of Water above Gas for Improved Sweep in Gas EOR: Non-uniform Injection and Sweep
Author	:	Adhitomo Sulistyo
Date	:	31st July 2017
Professor	:	Prof. Dr. W. R. Rossen
Supervisor	:	A. A. A. Hussain MSc
Postal Address	:	Section for Petroleum Engineering
		Department of Geoscience and Engineering
		Delft University of Technology
		P.O. Box 5028
		Netherlands
Telephone	:	(31) 15 278 1328 (Secretary)
Telefax	:	(31) 15 278 1189

Acknowledgements

The thesis committee has patiently guided me through the last two quarters until the completion of my thesis. Thank you to Prof. Rossen for being my supervisor and accepting me to be the student to carry out the project. Being the chair of the Petroleum Engineering section, even though he was very busy, he had always allocated adequate time to give advice and fuel me with countless suggestions for the project through the crucial bimonthly meetings. I would also like to thank PhD student, Ahmed Hussain for being the direct supervisor for this project and regularly providing ideas to run the different types of simulation.

Thank you to Dr. Voskov for the recommendation of using a different type of perturbation. Not to mention all the trouble that Li Longlong, one of his exchange PhD students, had to go through to help me out with the alternative simulation method. Although we were unable to incorporate the results because of the complications in running the simulator with my inputs, I had learned a lot, and I really appreciate the help and all the long hours of troubleshooting together.

I would like to express my deepest sense of gratitude to all the committee members for spending their valuable time to read, review, and evaluate the thesis.

I also want to thank all the lecturers and tutors for their sharing of knowledge throughout the two years of study at TU Delft. This masters study has proven to be challenging, yet rewarding. I hope this will provide an opportunity for a better career development. Thank you to all my friends who have made it such a pleasant experience to live in the Netherlands.

Finally, I would like to dedicate this thesis to my family, especially my wife, whom was pregnant and gave birth to my first child, Aisha, during the duration of the project. I was not able to be together with my wife for the nine months, but I was fortunate to be present during the delivery of the baby. Also to my mother and father for all their prayers such that everything goes well with my studies.

Abstract

One proposed method to delay the onset of gravity segregation between water and gas in enhanced oil and gas projects and extend the period of effective macroscopic sweep in "SWAG" is by separating the injection wells into two parallel horizontal wells (Stone, 2004). In this "modified SWAG", the water injection well is aligned at a distance above the gas injection well, and both water and gas are pumped simultaneously to displace the reservoir fluids. The significant density difference between the fluids and the ensuing counter-direction flow impede the segregation process.

Initially Rossen et al. (2007) investigated the effectiveness of the technique based on 2D modelling and found that it increased the fluid segregation length. Van der Bol (2007) and Jamshidnezhad et al. (2010) broadened the scope of study and observed a non-uniform gas injection profile and volumetric sweep in 3D. Injection instability occurred in most of the simulation cases, despite the assumption of an ideally homogenous reservoir in the model. Mahalle (2013) identified several factors that triggers instability such as gas saturation and relative permeability behaviors in adjacent grid blocks. Since the instability was found to originate in the near-wellbore region, local grid refinement was applied along the entire length of the horizontal well, with more uniform gas-injection profile observed. Using a different reservoir simulator, Ranjan (2015) extended the previous study by checking again the effect of local grid refinement. The result, however, contradicts with the preceding finding. Grid refinement near the injection well did not improve stability in Ranjan's study. The author also checked the effect of gas injection rate on the non-uniformity. Again, contradictory results were observed. While Ranjan reported that doubling the gas injection rate promotes non-uniform behavior, the earlier study obtained the opposite outcome.

This thesis extends the previous studies by examining other parameters that may influence non-uniformity. We developed a method to quantify non-uniformity by calculating the coefficient of variation and max-min ratios for gas injection rate along the well. We looked at the effect of changes in well placement, reservoir properties, reservoir boundaries, reservoir fluids and operating constraints. We also fundamentally modified how the perturbation is applied along the gas-injection well by altering the skin factor while maintaining constant permeability. Results show that the type of perturbation significantly effects the non-uniformity of gas injection. We believe that perturbing permeability promotes the uniformity of gas-injection rate because of flow to neighboring grid blocks, and thereby more simulations are seen to be uniform compared the results with perturbation in skin factor. The results from this study suggests that non-uniformity is associated to the feedback between gas injection rate, water saturation and gas relative permeability, which is shown by the gas injection rate to vary more than proportionally to permeability or skin, even in relatively uniform cases. The effect of adjacent grid blocks also plays a crucial role, as we can see from the different results between the two types of perturbations. Finally, the mobility ratio of the fluids strongly influences the occurrence of the instability.

Table of Contents

List of tables and figures

1. Introduction

1.1 Literature Review

Production of hydrocarbons from oil reservoirs is categorized into three main production stages. The initial or primary production phase is characterized by recovery by means of reservoir pressure. In this case the pressure contained in the reservoir is sufficient to lift fluids out of the well. The secondary production stage involves the injection of fluids such as water, to maintain reservoir pressure, and thereby sweep the remaining oil out of the reservoir. The tertiary stage improves recovery by altering the resident fluid properties for a more efficient extraction. This is also known as Enhanced Oil Recovery (EOR). One promising subclass of EOR is gas injection. The gas can be natural gas, nitrogen, or even carbon dioxide.

Table 1: Hydrocarbon production stages

Production Stage	Method	Example
Primary	Natural reservoir energy	Water drive, gas drive, artificial lift
Secondary	Fluid injection to maintain reservoir pressure	Water injection
Tertiary / EOR	Modify reservoir fluid properties	Thermal recovery, Chemical Injection, Gas Injection

Recovery factor is dependent on variables such as microscopic and macroscopic displacement efficiency. Unlike water flooding, which has a typical microscopic displacement efficiency of less than 70% due to capillary effects, the efficiency in gas floods is close to 100% (Muggeridge et al., 2014). However, gas EOR suffers from poor macroscopic displacement efficiency. Gravity segregation causes the gas to flow at the top of the reservoir, leading to poor hydrocarbon sweep. Therefore, gas injection alone is not an efficient and effective method for EOR (Hustad & Holt, 1992).

Introduction to SWAG

One way to improve the sweep efficiency of gas EOR is by combining gas injection with water injection. Some of the variations are Water Alternating Gas (WAG), Simultaneous Water and Gas (SWAG), and modified SWAG injection. WAG injection is defined as a process of injecting water and gas slugs in volume ratios of 0.5:1 to 4:1 (Panda et al., 2010). Compared to conventional waterflood systems, the recovery performance can reach up to 40% depending on the slug ratio (Panda et al., 2010). SWAG involves the co-injection of water and gas through a single well. It is anticipated that the fluid mixture will have a lower mobility in the mixed zone and prevent viscous fingering, which is a typical issue in water flooding (Mai & Kantzas, 2009). The mixed zone is defined as the zone in the reservoir where both and gas are flowing (***Figure 1***). Beyond the mixed zone, there is the override zone where only gas is flowing at the top, and there is the underride zone where only water is flowing at the bottom (Rossen & van

Duijn, 2004). A more recent study by Stone (2004) suggests a different approach in SWAG, which Algharaib et al (2007) later named “modified SWAG”. Instead of injecting the fluids from a single well, water and gas are injected separately from two horizontal wells. Gas is injected at the bottom of the reservoir and water is injected at the top of the reservoir. Therefore, gravity works in favor of the sweep, as the heavier water tends to flow downward and the gas flow upward. This counter-current flow results in a better sweep efficiency, and consequently oil recovery compared to SWAG (Rossen et al., 2010).

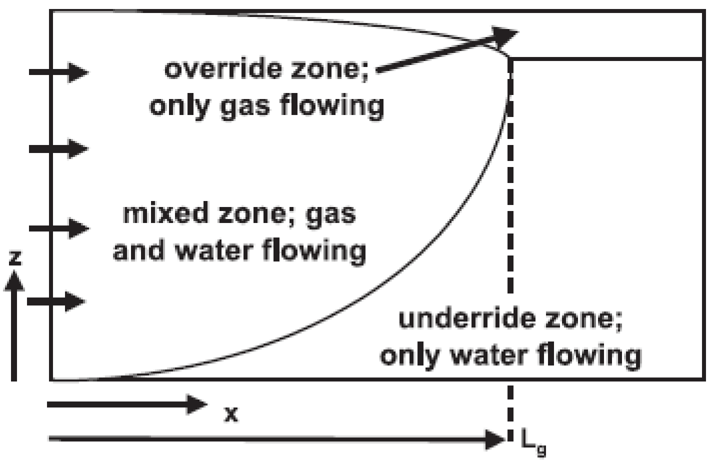

Figure 1: Schematic of three uniform regions in the reservoir (Rossen & van Duijn, 2004). L_g represents the length of the mixed zone, often referred to as the segregation length.

Extensive studies on the sweep efficiency of modified SWAG were carried out. Stone (2004) initially presented the method in 2D. Rossen and Shen (2007) found that the method to be superior compared to the conventional SWAG injection. The effectiveness of SWAG injection is related to the achievable volume covered by the mixed zone and its segregation length, which is the distance at which water and gas completely separates in the reservoir. The segregation length achieved with modified SWAG injection was found to be longer than with SWAG injection. Furthermore, the positioning of both horizontal wells is also an imperative factor as it affects the shape of the mixed zone and ultimately the volume swept by the injected fluids (Stone, 2004). Ideally when the gas injection well is placed at the bottom of the reservoir, one might expect that it results in a better sweep.

Previous studies on non-uniform injection in modified SWAG injection

Previous studies on the modified SWAG prior to 2007 were limited to two dimensional simulations. Van der Bol (2007) was the first person to report the occurrence of non-uniform gas injection profile in 3D simulation. Specifically, she studied the case where water and gas are injected with two separate horizontal wells. Compared to the 2D simulations, bypassing of gas and water occurs in 3D simulations, instead of segregation by means of countercurrent flow of both fluids. The gas injection profile along the horizontal gas injection well was non-uniform, even though the simulations were performed in homogenous reservoirs. Unlike the 2D simulation where the horizontal well is represented as a single point, in 3D simulation the injection well is present in multiple interconnected grid blocks on the x-y plane. In this configuration, there are multiple flow paths for the gas to exit the injection well, which may lead to asymmetric injection. Van der Bol (2007) also found that the onset of non-uniform injection can be accelerated by perturbing the permeability of the grid-blocks where gas injection occurs by ±10%.

When gas injection occurs non-uniformly along the injection well, the gas macroscopic sweep efficiency is reduced, and thereby recovery factor is less than expected. Instead of achieving an almost piston-like displacement of the oil, results show that the gas moves through the reservoir primarily along one path, in a manner similar to viscous fingering. Therefore, several authors followed up the initial study to understand the cause of instability in gas injection and find measures to minimize the occurrence.

Jamshidnezhad et al. (2010) studied the effect of several simulation parameters on the onset of gas-injection non-uniformity, using the CMG STARS simulation software. In the paper, it is suggested that if gas-injection instability develops, there is a tendency for gas to predominantly exit from a single grid-block after steady state condition is reached. Results show that uniformity of gas injection correlates positively with increasing the total injection rate and decreasing the vertical gap between the two injection wells. Moreover, Jamshidnezhad et al. (2010) reported that uniformity can be improved somewhat by segmenting the horizontal well and injecting separately into each segment. Instead of having a single injection point, he separated the injection well into three segments and had the rate individually controlled in each segment.

Mahalle (2013) followed up the study with a master thesis and validated some of the simulations performed by Jamshidnezhad (2010). Although a different simulator was used, the Shell in-house simulation software MoReS, similar results were obtained to what was found by Jamshidnezhad (2010). The vertical distance between the two injection wells is a parameter that effect the instability. As the distance is reduced, a more uniform gas-injection profile along the injection well is observed. The same effect as reported by jamshidnezhad is also obtained when segmentation is done. To further understand the gas injection non-uniformity, Mahalle (2013) performed extensive trials that investigate, among other factors, grid refinement, adjustments to fluid properties, and grid-block interactions. It was found that a finer grid leads to a more non-uniform gas-injection profile. While injection rates were still observed in the base case in every injection grid block, in the finer-grid simulation, where the number of grid blocks was doubled, the injection ceased completely in some grid blocks. Local Grid Refinement (LGR), however, yielded opposite results to those in previous studies When the number of grid blocks in the injector wells was refined by a factor of three, a more-uniform injection profile was obtained. The author also showed the effect of adjacent grid blocks on injection profile. Without lateral connectivity with neighboring blocks, a better distribution of gas injection is attained. Mahalle (2013) also investigated the relation of the gas-injection non-uniformity to the changes in gas saturation and thereby gas relative permeability, by altering the gas saturation exponent in the Brooks-Corey relation. He found that the Brooks-Corey relation has little effect on the uniformity of gas injection itself; rather there was a change in the location of the grid block with the highest gas flux.

Ranjan (2015) continued the 3D-simulation study using the Eclipse simulator, which is the same simulator that was used in the initial research by Van der Bol (2007). Ranjan (2015) reported that the increase in total injection rate does not lead to a more-uniform injection profile, but the opposite outcome, which contradicts the finding by Jamshidnezhad et al. (2010). However, the study confirms that increasing the number of segments along the horizontal gas injection well leads to improved uniformity. Comparable results to the study by Mahalle (2013) were also obtained when lateral connectivity was removed. However, a different result was observed when Ranjan (2015) modified the gas-saturation exponent. Injection was more non-uniform when the exponent was increased, whereas in Mahalle's case the location of maximum gas injection rate has changed from the heel to the toe. Additionally, the author showed that reduction in gas viscosity has a positive effect on the uniformity of gas injection.

It is worth noting that the researchers used different software to run their simulations. Both Van der Bol (2007) and Ranjan (2015) used Eclipse, while Jamshidnezhad et al. (2010) used CMG STARS, and Mahalle (2013) used MoReS. Although the base case for each researcher was similar, the outcome from the simulations was not the same in every case. **Table 2** summarizes the simulations run by each of the researchers after Van der Bol (2007) and the outcomes. The three researchers focused on the different parameters that lead to changes in uniformity of gas injection.

Table 2: Comparison of parameter impact on gas-injection profile when performing modified SWAG flood, by Jamshidnezhad et al. (2010), Mahalle (2013), and Ranjan (2015).

Change made from Base Case	Jamshidnezhad et al. (2010)	Mahalle (2013)	Ranjan (2015)
Increase gas injection rate	+	NT	-
Reduce vertical distance between wells	+	+	NT
Increase number of segments	+	+	+
Fine grid modelling	NT	-	NE
Local Grid Refinement around injection wells	NT	+	NE
Remove lateral connectivity of grid blocks	NT	+	+
Reduce gas saturation exponent	NT	NE	+
Reduce gas viscosity	NT	NT	+

+ (more uniform)
- (less uniform)
Not Tested
No Effect

Well Model

Numerical reservoir simulation software is based on a mathematical model. The accuracy of the numerical simulation is dependent on the ability of the model to properly describe the subsurface transport phenomenon from the production into the reservoir for fluid injection and from the reservoir to the production well for fluid production. Variations in the model and its numerical simulation may lead to different results as depicted in **Table 2**, in the comparison of previous studies on modified SWAG flood.

One of the determining factors in the simulation model is pressure. It is understood that a pressure gradient is necessary for a fluid to flow through the reservoir. For the simulator to accurately model the changes in pressure, the size of grid block should ideally be small throughout the reservoir. Finer gird size allows better description of heterogeneity in the reservoir, and better resolution of phase behavior and fluid fronts (Mattax & Dalton, 1990). However, we are constrained by computational power, and therefore running simulations with very small grid blocks in a relatively large reservoir will be unpractical. One way to solve this problem is by local grid refinement. Since the steepest pressure gradients are near the production and injection wells, grid blocks near the wells can be set to a smaller size compared to the rest of the reservoir.

Well equations are developed to compute the dynamic bottom-hole pressure at a given fluid injection or production rate. Alternatively, the equations can be used to calculate the rates when the bottom-hole pressure is given by the user. In this study, we used the Peaceman (1978) equation for single-phase flow in Cartesian grids using finite-difference methods. Peaceman (1978) showed that when steady state is reached, the grid block pressure is related to the wellbore pressure at an equivalent radius r_e. By implementing various analytical and numerical approaches, Peaceman (1978) inferred that, for a square grid block in 2D, the equivalent radius is approximately 0.2 times the grid size *h (length and width)*. For example, given a grid size of 1 m, the numerically calculated difference between well and grid-block pressures will be that for steady-state flow out to an equivalent radius of 0.2 m.

The well model developed by Peaceman was extended by further studies to take into account different situations such as multiphase flows and horizontal wells. Babu et al. (1991) derived the analytical equation to determine the effective radius in the grid block containing the well. This radius is required to draw the relationship between wellbore and grid-block pressures. Babu et al. (1991) modified Peaceman's equation such that it is generally valid not only for vertical wells with high permeability anisotropy and rectangular drainage area, but also horizontal wells at any location and aspect ratio of its corresponding drainage area.

To achieve a better representation of the subsurface, the presence of different fluids has to be taken into account into the model. The coexistence of oil, water, and gas is bound to affect the flow of one another in terms fluid pressure and rates. Several techniques that are currently implemented in multiphase flow simulations include Implicit Pressure-Explicit Saturation (ImPES), Simultaneous Simulation (SS), Adaptive Implicit, etc. (Chen et al., 2006)

Despite the limitations associated with the Peaceman's model, it is widely used in current commercial simulators. Dietrich and Kuo (1996) found that the model results in incorrect prediction of well productivity when the reservoir is modeled with a uniform coarse grid. Better results were obtained when the reservoir was modeled with a non-uniform fine grid. Therefore, several assumptions need to be made when applying the Peaceman model. These assumptions include uniform grid, homogenous reservoir, single-phase flow, steady state condition, and a cell-centered and isolated well (Wan et al., 2000). The isolation here is in terms of position relative to the boundaries and other wells. Ideally, the well should be more than five grid blocks from the boundaries and more than ten grid blocks from the nearest well (Aziz & Settari, 2000). Previous studies by Jamshidnezhad (2010), Mahalle (2013), and Ranjan (2015) were did not fully meet the isolation requirement. Although the injection and production wells were sufficiently far from each other, they were located adjacent to the boundaries. Therefore, in this study we aim to tailor the simulation inputs to minimize potential errors in the results.

1.2 Objective

The literature review suggests that the root cause of the occurrence of non-uniform gas injection in modified SWAG technique has not been identified. This thesis extends the previous studies by examining several different parameters, which are classified into five categories: production-well placement, reservoir boundary, reservoir properties, reservoir-fluid properties, and production parameters. We develop a method to quantify the degree of non-uniformity by using indicators such as the gas injection rate coefficient of variation (CV) and maximum-minimum ratios. Moreover, we study the effect of skin perturbation in place of permeability perturbation, and how it changes the non-uniformity of gas injection.

2. Research Methodology

2.1 Base case Reservoir Model Description

Boundary Conditions and Grids

The reservoir is modeled as a 3D rectangular box with sealed boundaries on all sides. Fluids enter and exit the reservoir only through the injection and production wells, respectively. The reservoir dimensions are 64 X 60 X 40 m. The grid resolution is 32 X 15 X 30. The reservoir shape and size are chosen to enable comparison with previous studies. This grid serves as the base case for subsequent simulations. The model is constructed from regular grids, and the size of each grid block is 2 X 4 X 1.5 m, except for the top five grid blocks, which are 0.5 m thick, to allow finer resolution and thus more accurate analysis of the override zone at the top of reservoir (**Figure 2)**.

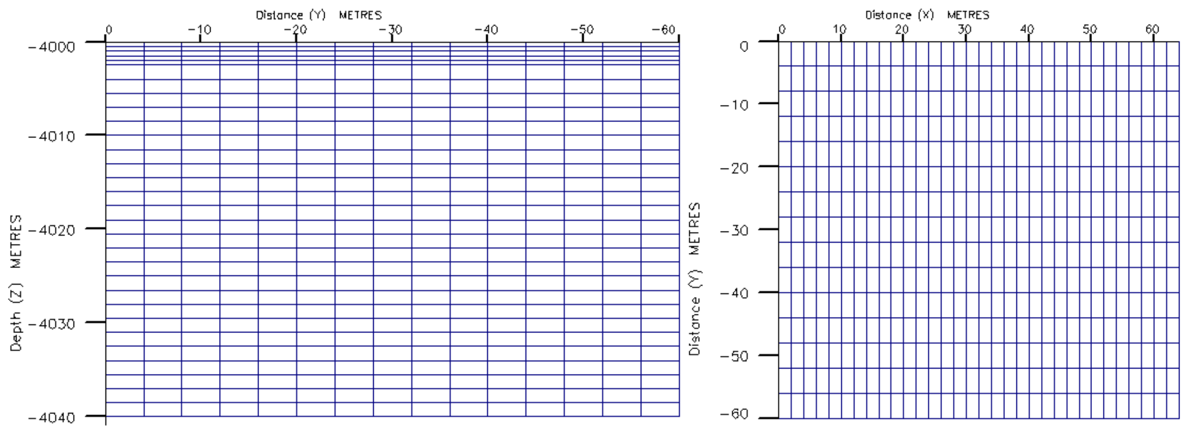

Figure 2: Reservoir grid: cross section along x-axis (left); along z-axis (right)

Wells

The implementation of modified SWAG injection is done by drilling two horizontal injection wells, opposite to a vertical production well (**Figure 3**). The horizontal water-injection well is located at coordinates (x=1, y=1 to 15, z=17), and the horizontal gas injection well is located at coordinates (x=1, y=1 to15, z=30). The vertical production well is located at the following coordinate (x=32, y=7, z=1 to 30), which is offset by one grid block from the central plane of the reservoir in the y-direction. The location of these wells being so close to the boundary does not entirely satisfy the limitations in the Peaceman's model, and therefore it is expected that results may be less accurate. Open-hole completions are assumed throughout the lengths of each well to minimize restriction of fluid flow. The wellbore diameter for each well is 0.2 meters. Friction inside the well is set to zero to simplify the model and avoid potential pressure build-ups which may contribute to the non-uniformity of injection. Friction in a real well would tend to favor injection from the heel, but we are interested in instabilities leading to non-uniform injection even in the absence of this effect.

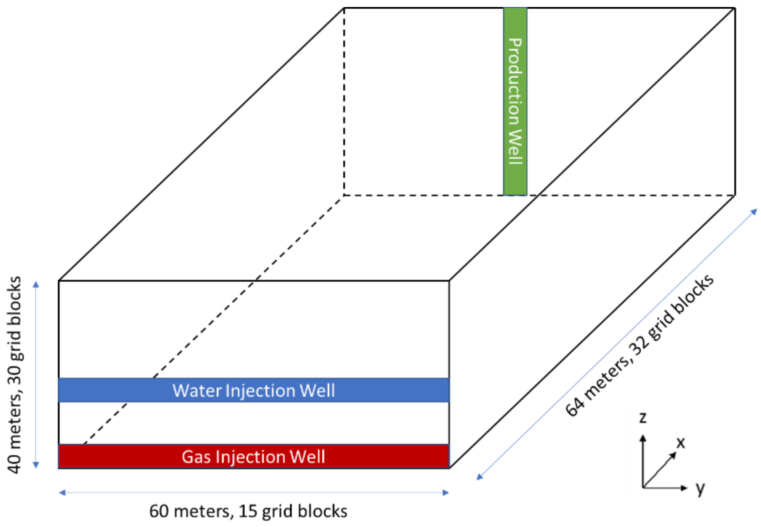

Figure 3: Well configuration and reservoir dimensions

It is worth noting that the location of the production well is not exactly in the middle of the reservoir in the y-direction. It is located at the 7th grid block along the 15 grid blocks of reservoir. With the reservoir length width of 60 m, an offset of one grid block translates to 4 m distance from the central plane.

2.2 Reservoir and Fluid Properties

The reservoir is set to be homogenous with a horizontal permeability of 1000 mD, vertical permeability of 210 mD, and porosity of 25% in every grid block. In the last grid sheet, which includes the production well, horizontal permeability is set to 10,000 mD to represent an open boundary, and vertical permeability is set to a small value of 0.01 mD to induce horizontal flow exclusively towards the production well. This is to simplify the model and prevent cross flow in the vertical direction in the last grid sheet, particularly in the grid block that contains the production well. Homogeneity throughout the rest of the reservoir is applied to rule out the possibility of non-uniform injection caused by reservoir heterogeneity. However, based on the study of Van der Bol (2007), small permeability perturbations ($\leq$ 10%) are introduced on the injection-well grid blocks to accelerate the onset of instability. Without perturbations, van der Bol found that non-uniformity develops over a longer period since it is initiated only by computational round-off errors. Therefore, this perturbation was introduced to reduce computational time of each simulation. Alternatively, in some cases, perturbations were introduced in the skin factor (**Figure 5**) instead of permeability (**Figure 4**). By perturbing the skin, we avoid variation in transmissibility between neighboring grid blocks, which occurs when the permeability is perturbed.

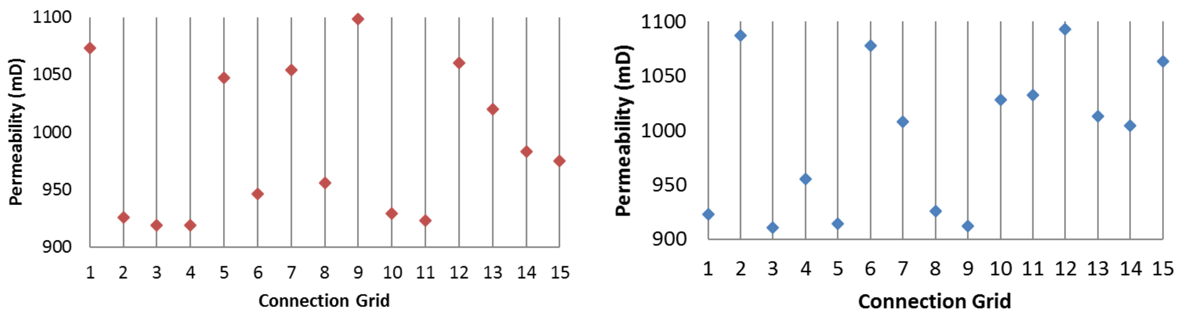

Figure 4: Horizontal permeability along the gas-injection well (left) and water-injection well (right).

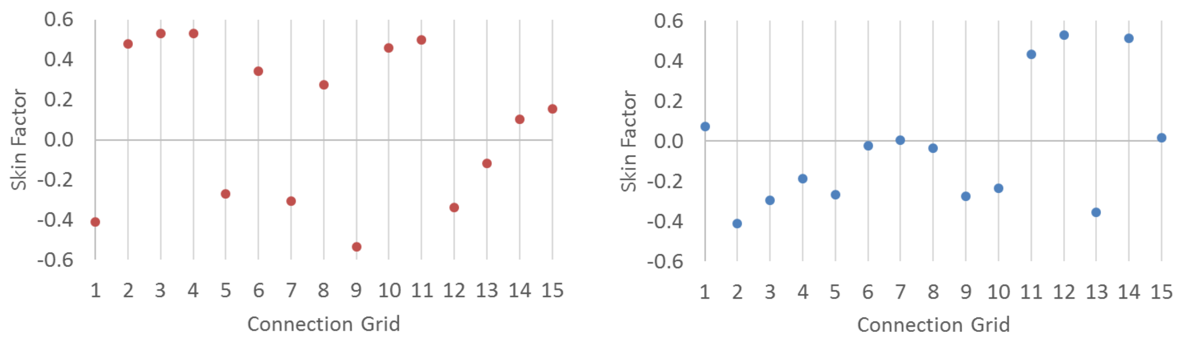

Figure 5: Skin values along the gas-injection well (left) and water-injection well (right).

For comparison with the previous studies, analysis is done at steady-state condition. Similarly, we have specified the reservoir to contain no oil as it does not fundamentally affect the characteristics of fluid segregation. Moreover, one might assume that mobile oil is quickly displaced from the vicinity of injection wells. Due to the absence of oil, the simulations use a two-phase relative permeability model. The initial gas saturation is 15%, in the reservoir is equal to the irreducible gas saturation. The Corey exponent for gas is 2, and end-point relative permeability of gas is 1. The connate water saturation is set to 20%, the Corey exponent for water is 2.5, and end-point relative permeability of water is 0.3. These parameters create the relative-permeability functions for the base case shown in ***Figure 6***, which corresponds to those in Mahalle (2013) and Ranjan (2015).

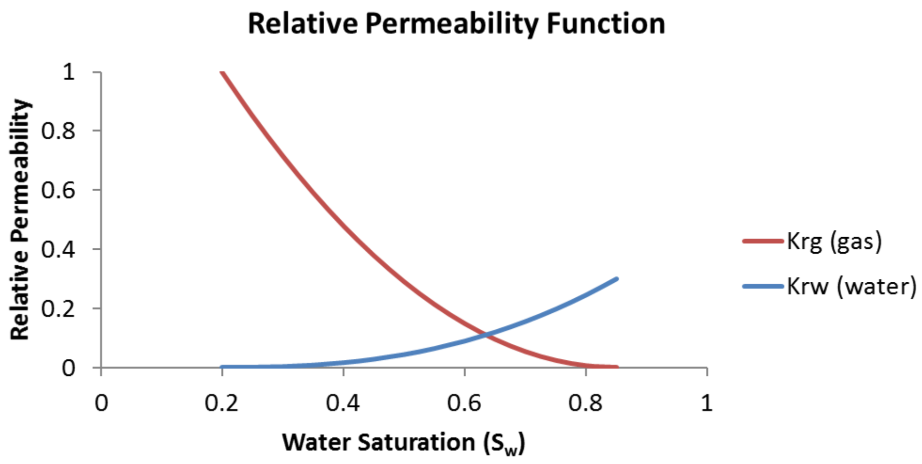

Figure 6: Water-gas relative permeability function

In previous studies, reservoir fluids were set to be incompressible to simplify the problem. Since Eclipse does not allow zero compressibility, we have specified a small value of 10^{-5} bar^{-1} to represent incompressible fluids. Although the compressibility is almost zero, there still exists a difference in reservoir and surface volumes. This is described by the gas formation volume factor B_g, which does not change much with pressure due to low compressibility.

2.3 Operating Constraints

The reservoir is set to an initial pressure of 140 bars at the top reservoir boundary with vertical variation of pressure due to the water hydrostatic gradient. The production well is pressure-controlled with the bottom-hole pressure set to 140 bars. Initial reservoir pressure and injection-well bottom-hole pressure are equal to avoid a sudden increase in initial production rate, and to ensure that the total injection rate is equal to total production rate. Total injection rate is set to 220 Sm^3/day, with water representing 29% of total injection rate (63.8 Sm^3/day) and gas the remainder (156.2 Sm^3/day). These numbers are equivalent to the values used by Jamshidnezhad (2010). Because the gas formation volume factor at 140 bar is 0.129, the equivalent rate of gas being injected into the reservoir is around 20.2 Rm^3/day. Therefore, the total injection rate at reservoir conditions is 84 Rm^3/day. Capillary effects are neglected. Unless mentioned otherwise, simulation time is one year, as we have observed that steady state is achieved within this time frame, and the simulation results then are comparable to longer periods.

2.4 Quantifying the degree of non-uniformity

In previous studies by Jamshidnezhad (2010), Mahalle (2013), and Ranjan (2015), non-uniformity was determined through qualitative judgement of the gas-injection profile. The precise distinction uniform and non-uniform gas-injection have also not been established. In this study, we utilize several numerical indicators to quantify non-uniformity. The first indicator is coefficient of variation (CV) and maximum-to-minimum ratio of gas injection rate. The CV is defined as the ratio of standard deviation to the mean value. Results of simulation can be described as becoming less uniform or more uniform depending on the change in magnitude of CV. The higher the CV and gas injection rate max-min ratio the higher the non-uniformity, which is normally indicative of the presence of an extremely high injection rate in one grid block.

Another indicator of non-uniformity is the strength of correlation between gas injection rate and perturbation. We observe that cases with relatively uniform gas injection display strong correlation, while cases which are non-uniform display weak correlation. The correlation is determined by comparing the data spread relative to its the linear best-fit curve. Specifically, we consider the 95% confidence interval of the slope due to the limited number of data available for regression. If the summation of slope ± confidence interval includes zero, this means that there is a high probability that there is no correlation between the gas injection rate and perturbation. In this case, the variation in gas injection rate is probably random, and the gas-injection profile is considered non-uniform.

3. Results and Discussion

The focus of this thesis is to study the occurrence of non-uniform gas injection in modified SWAG. Van der Bol (2007) initially discovered the development of non-uniform gas injection in a 3D-reservoir simulation. The non-uniformity was present even in completely homogenous reservoir without any perturbation. Jamshidnezhad (2010) began investigating potential causes of the phenomenon by running simulations with different parameters including total injection rate, injection well placement and segmentation. Mahalle (2013) validated several results from the previous researcher and explored other parameters such as fine-grid modelling and the effect of the exponent in the gas relative permeability expression. Ranjan (2015) continued the study by validating almost all the cases which were tested by Mahalle (2013) and Jamshidnezhad (2010). Validation is an important step to make sure the output from the different simulators used by all the researchers are comparable. Comparison of results show that the output from the simulators are not always the same, albeit the same inputs are used to replicate the reservoir and fluid model. In this study, we begin by validating the base case from the previous work.

Since we are using the same simulator as Ranjan (2015), we can quickly run the simulation with the same dynamic model to validate the output. Unlike Ranjan, we decided to randomize the permeability distribution in both the water- and gas-injection wells, as illustrated in **Figure 4**. We believe that having different permeability distributions gives a check on the effects of the perturbations and avoids potential bias to the results.

In other cases, we perturbed the wellbore skin factor, as illustrated in **Figure 5**. Unlike grid-block permeability, this perturbation in skin has no direct impact on flow between neighboring grid blocks. The magnitude of skin perturbations were set in such a way that the same injectivity index was achieved as with permeability perturbations.

Changes in parameters are classified into several categories: well placement, reservoir properties, fluid properties, and operating constraints. Each category contains variables that are changed to test specific hypotheses. These parameters are modified individually, to simplify the analysis of results. Besides qualitative analysis of the uniformity of gas injection, we report the quantitative indicators described above.

3.1 Cases with perturbed permeability

3.1.1 Base case

The base case provides the benchmark for non-uniformity in our simulations. It is composed of the exact same dynamic model as Ranjan (2015). Fluids are injected through two vertically separated horizontal wells at a constant total rate of 220 sm^3/day (84 Rm^3/day) into a reservoir with 38,400 m^3 pore volume, based on 64 X 60 X 40 m bulk dimension with 25% porosity. At the bottom of the reservoir gas is injected, while in the middle of the reservoir water is injected at 0.29 fraction of the total volumetric rate at reservoir conditions. Initial reservoir pressure is set to 140 bars. The production well is constrained to 140 bars bottom-hole pressure (BHP) to avoid a sudden initial spike in production rate due to a large pressure differential between the reservoir and well pressures, as was observed when BHP was set to 60 bars in Ranjan (2015).

Figure 7 depicts the gas injection rate in the well grid blocks versus the permeability in the grid-blocks after one year. Gas injection rate in individual grid blocks is initially distributed nearly equally, but develops a non-uniform distribution as the flow reaches steady state. The coefficient of variation (CV) for this case is 1.398. The theoretical maximum CV that can be attained for the worst case of non-uniformity when all flow comes out of one grid block is 3.87. Subsequent cases with more than 1.398 are more non-uniform, while cases with less than 1.398 are considered more uniform.

One hypothesis is that non-uniformity is caused by asymmetry in the pressure profile due to the location of the production well. It is understood that flow always occurs from the high-pressure to low-pressure regions. The reservoir pressure profile is determined by the geometry of reservoir and well placement relative to the boundary. Since the lowest pressure in the end sheet of grid blocks occurs in the production-well grid blocks on the 7th column of grid blocks in the y-direction (**Figure 8**), if there are any variation in gas injection flow rate, the highest magnitude should be at the 7th grid of gas injection well, not the 1st. However, the pressure profile along the injection well grid blocks is different than the production side, with the highest pressure in the 15th grid block and lowest in the 1st, which explains the tendency of gas to flow from the heel. Nevertheless, the pressure difference between the grid blocks is small (< 1 bar), so we did not expect such large difference in gas injection rate.

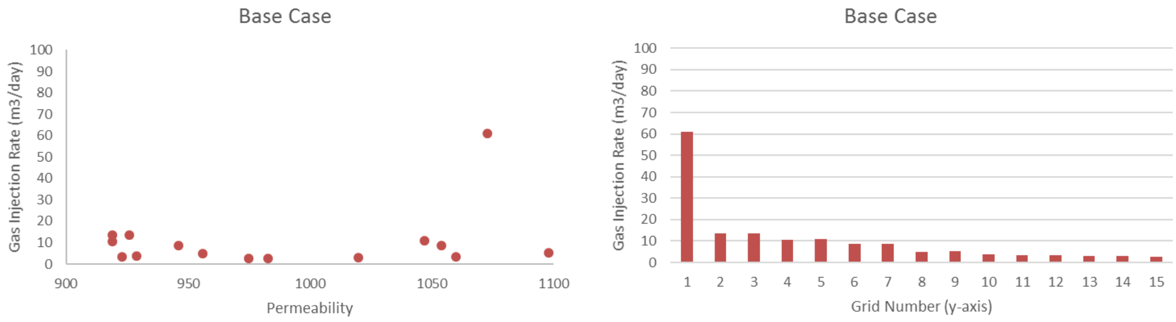

Figure 7: Permeability-perturbation base case. Left: Correlation between gas injection rate after one year and grid-block permeability. Right: Gas-injection-rate profile along well.

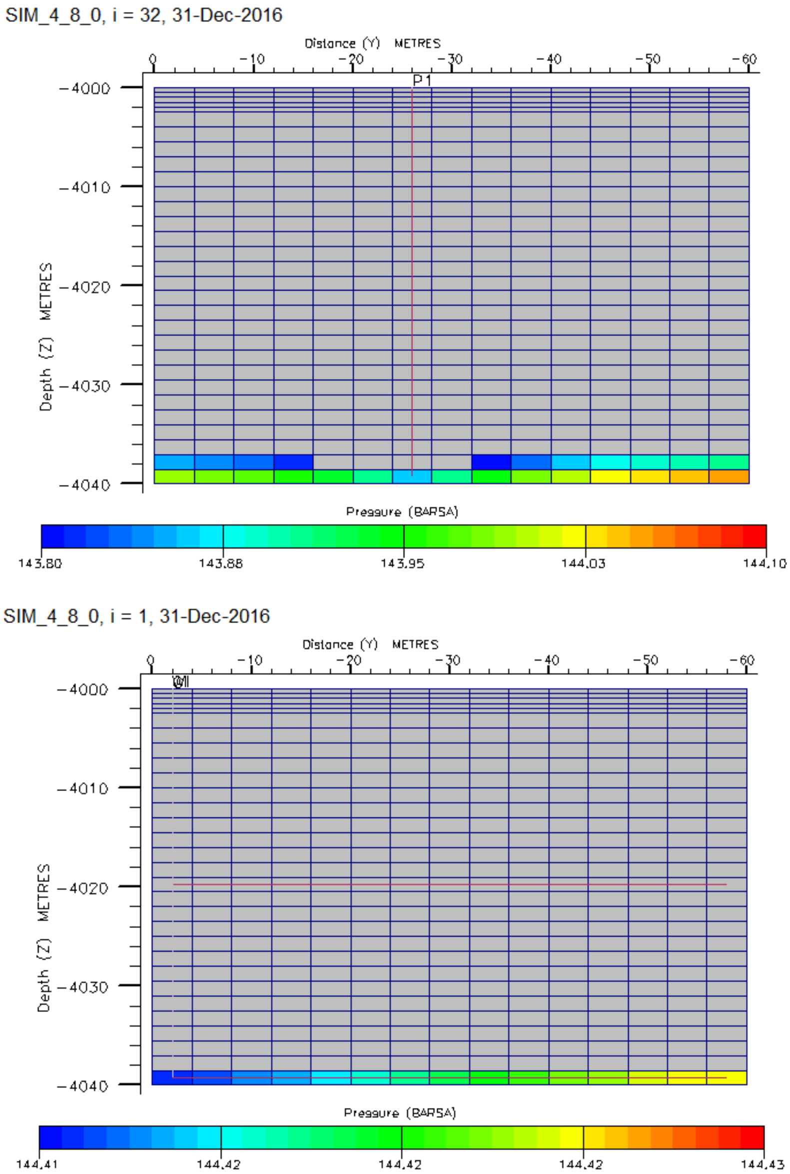

a

b

Figure 8: Pressure distribution at the end of simulation at t=365 days with the production well on the 7th grid block in y-direction. Front view (y-z plane) a) at the production end-sheet of grid blocks, i.e. at x=32. b) at the injection side, i.e. at x=1.

3.1.2 Effect of production well placement

To validate the first hypothesis, we run several additional simulations by changing the position of the production well.

Production well exactly in the middle (8th grid block)

By placing the production well in the center of symmetry in y-direction, we set the distance to the boundaries to be equal on each side. This leads to a change in pressure gradient, and thus makes the gas injection rate more uniform as indicated by a CV of 0.261 and visual distribution of rate as shown in **Figure 9**. The pressure profile along the injection well at the first grid sheet at x=1 shows the same trend in pressure profile at the last grid sheet at x=32 along the grids in the y-direction. Conversely, the base case has different trends between the injection and production grid sheets. Furthermore, the pressure is no longer monotonically decreasing from heel to toe (**Figure 10)**, but relatively even such that there is no extremely high rate in one of the grid blocks. Although results become more uniform, it is not what as we expected in the hypothesis. A shift in production well to the 8th grid block should shift the highest rate to the injection grid with the highest permeability. The pressure gradient should be decreasing from each side of the reservoir towards the middle. An even pressure distribution should only be seen if there are multiple production wells, simulating an open boundary on the end sheet of the reservoir.

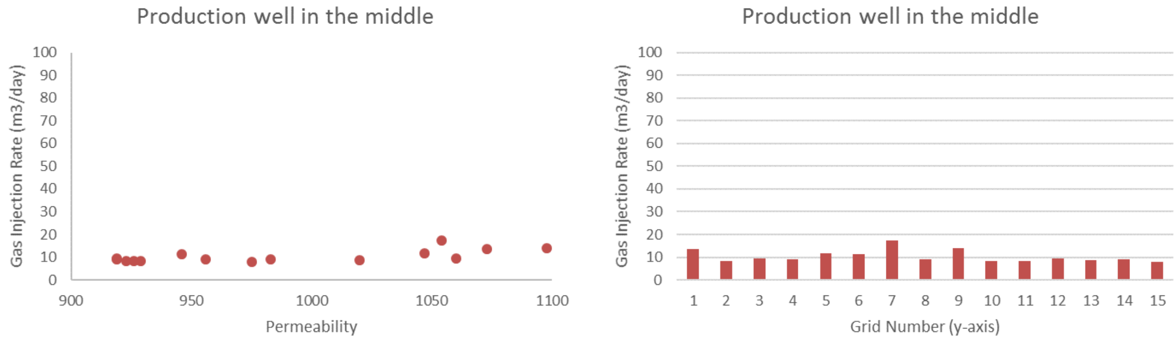

Figure 9: Permeability perturbation with production well on 8th grid block in the y-direction. Left: Correlation between gas injection rate and permeability. Right: Gas injection rate-profile.

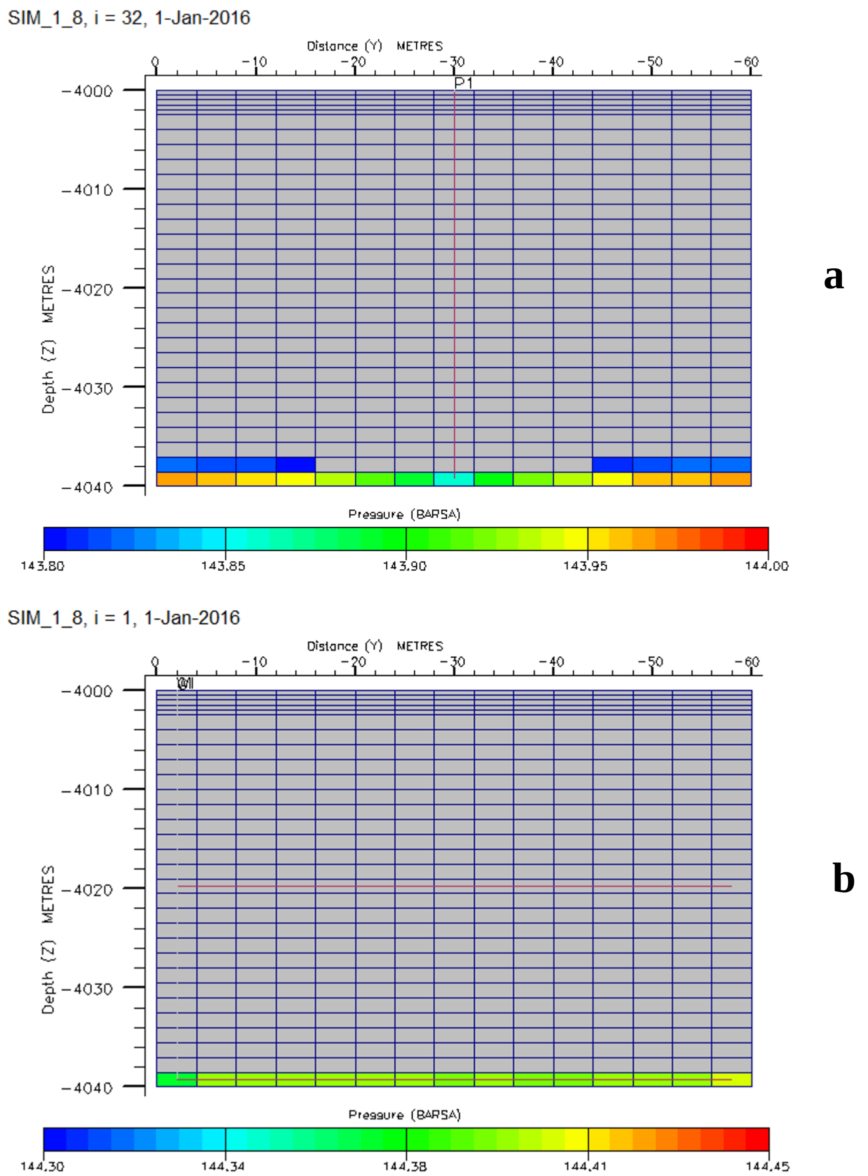

Figure 10: Production well in 8th grid block in y-direction. Front view (y-z plane). a) Pressure gradient at the production end-sheet / production side at x=32. b) Pressure gradient at the injection side at x=1. Both figures are at the end of simulation at t=365 days

15 vertical production wells

By placing 15 vertical production wells in the end-sheet, we create a zero pressure-gradient along the y-direction. This condition simulates an open boundary. Therefore, there should be no preference for the gas to flow into one of the grid blocks.

Figure 11 shows the simulation results with one production well in each of the 15 grid blocks in the y-direction at the end sheet. The distribution of flow rate is as expected. The CV is 0.247 which is almost identical as the previous case. The modest variation of injection rate among grid blocks is partly attributed to the differences in absolute permeability of the injection grid blocks. The magnitude of variation in gas injection, however, does not fully correlate to the permeability distribution, as we still can see deviations from the linear regression. Like the previous case, the reservoir configuration is now in perfect symmetry (except for the perturbed permeabilities along the injection well). The relative distances to the left and right boundaries are equal. Since there are multiple production wells, the pressure drop along grid blocks the y-direction is kept to a minimum or almost zero. Zero pressure gradient avoids preferential flow of the gas into one of the grid blocks by replicating flow to an open boundary.

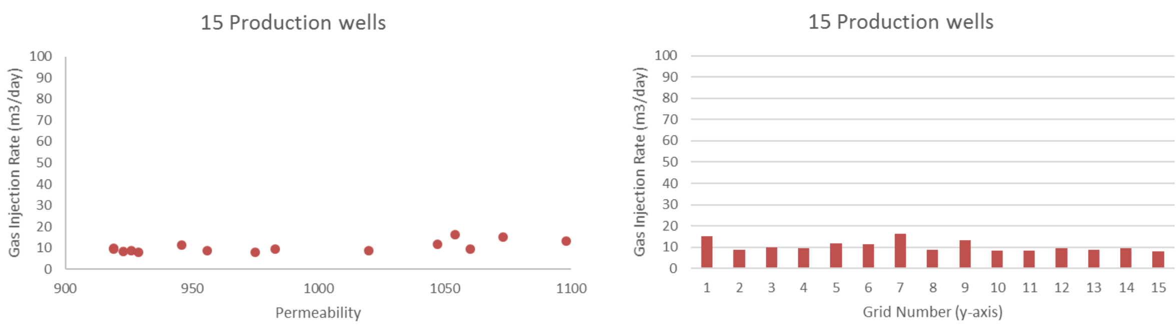

Figure 11: Permeability perturbation with 15 production wells. Left: Correlation between gas injection rate and permeability. Right: Gas injection-rate profile.

Alternatively, flow to open boundary can also be simulated by changing reservoir properties (**section 3.1.4**). Specifically, the end-sheet permeability can be increased to a much larger value compared to the general reservoir permeability. Increasing the end sheet permeability has a similar effect to having multiple production wells: it approaches the same pressure in every grid block in the last grid sheet. This brings us to the second hypothesis, that the presence of an open boundary at the production-well side increases uniformity of gas injection over having a single well there, especially if it is placed asymmetrically.

Production Wells on the 7th and 9th grid block

So far, we have tested simulations with either one production well and varying its position, or with 15 production wells. For this case, we have decided to place two production wells in such a way that symmetry is maintained. The wells are placed on the 7th and 9th grid blocks in the y-direction. This is to test whether the condition of non-uniformity is related to the boundary condition provided by the production well. Results in **Figure 12** show that the presence of a second well on the right-side counters the non-uniformity on the left, creating a more-uniform distribution of gas-injection rate. This suggests that the non-uniformity is increased by the boundary condition from the asymmetric positioning of the production well. It was expected that the highest gas injection rates are on the 1st and 15th grid blocks because both production wells are drawing the gas from each end of the injection well, as in the case if one production well is placed on either 7th or 9th grid blocks alone.

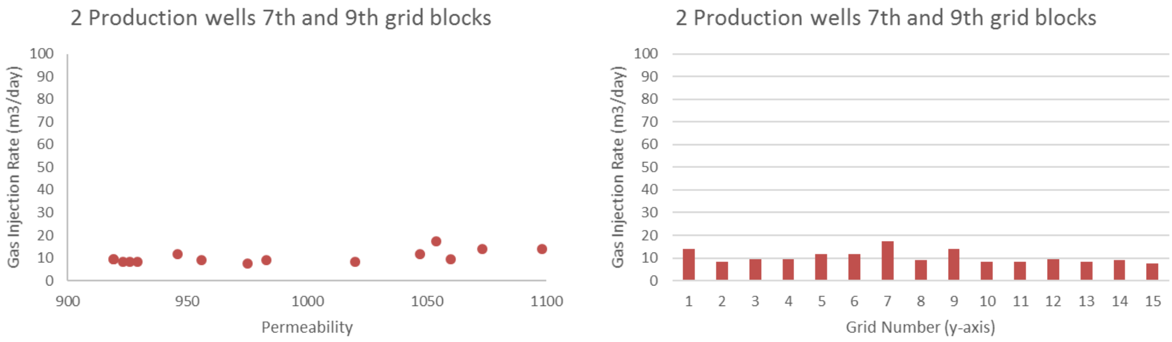

Figure 12: Permeability perturbation with two production wells, one on the 7th and the other on the 9th grid block. Left: Correlation between gas-injection rate and permeability. Right: Gas injection-rate profile.

3.1.3 Effect of changes in reservoir boundary

Aziz and Settari (1979) describe the ideal condition of the placement of the wells relative to the boundary and to each other, to obtain the most accurate results when using the Peaceman equation for injectivity. Therefore, in this case we satisfy the conditions by expanding the reservoir dimensions in all directions, while keeping the positioning and well dimensions the same. Specifically, the reservoir is extended in the x-direction by 20 grid blocks (10 grid blocks beyond the production well and 10 grid blocks beyond the injection wells), in the y-direction by 20 grid blocks (10 grid blocks beyond the heel and 10 grid blocks beyond the toe of the horizontal injection wells), and in the z-direction by 10 grid blocks (below the bottom of the reservoir). The total dimension is now 104 X 140 X 55 m and the grid resolution is 52 X 35 X 40. The comparison with base case dimensions is illustrated in **Figure 13**.

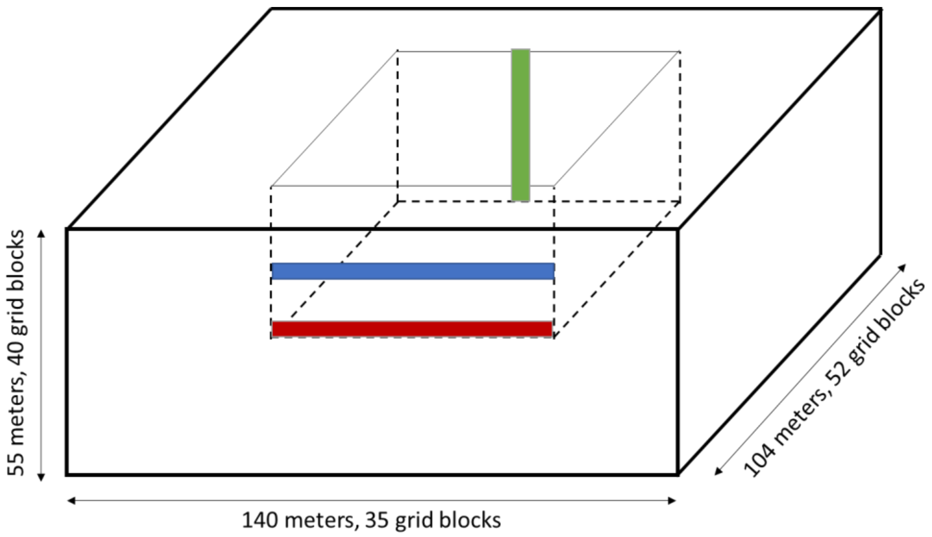

Figure 13: Reservoir expansion in all directions (not to scale). Well configuration and positioning is unchanged

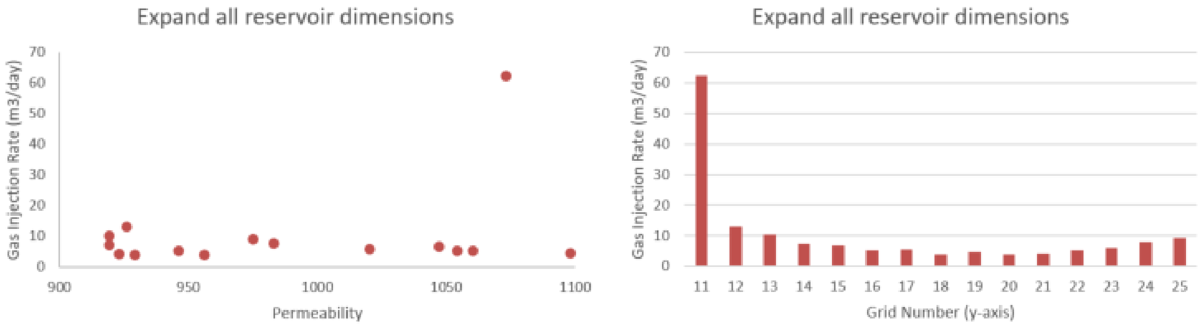

Figure 14: Permeability perturbation with expanded reservoir in all directions. Left: Correlation between gas injection rate and permeability. Right: Gas injection-rate profile.

Although we have satisfied the condition for Peaceman's model, the gas injection non-uniformity generally remains unchanged. We observe that there is slight change in gas injection-rate distribution (**Figure 14**) and a small increase in CV from 1.298 in the base case to 1.403. Therefore, the deviation in the base case from the assumptions of the Peaceman equation does not explain the occurrence of non-uniform gas injection in that case. In relation to well positioning, since the relative distance between the production well to the left and right boundaries is the comparable to the base case, there is no change in symmetry, and the result is as expected.

3.1.4 Effect of changes in reservoir properties

Increase permeability on ZY plane on the production-well side

In this case the end-sheet permeability is increased by a factor of 1000 from the base case. This high-permeability layer better mimics an open boundary by reducing the pressure drop along the y-direction, such that there is hardly any difference in pressure between the production well grid block and the other grid blocks in the same YZ plane. Theoretically, pressure drop should not be less than the case with multiple production wells (**Figure 11**) as this case is only an approximation to the open boundary. The approximation gets better with increasing the end-sheet permeability. The resulting CV is 0.244, which is slightly lower than the case with 15 production wells, which is not as expected. Theoretically, having multiple production wells should have the least pressure variation between grid blocks (i.e., zero), and thus should result to the smallest CV. **Figure 15** shows the distribution of gas-injection rate and correlation with permeability. Likewise, they show more-uniform gas injection than the base case, but, unexpectedly, slightly lower CV than the case of multiple production wells. We speculate that the small difference in flow rates observed in this case is related to the permeability perturbation at the injection-well grid blocks.

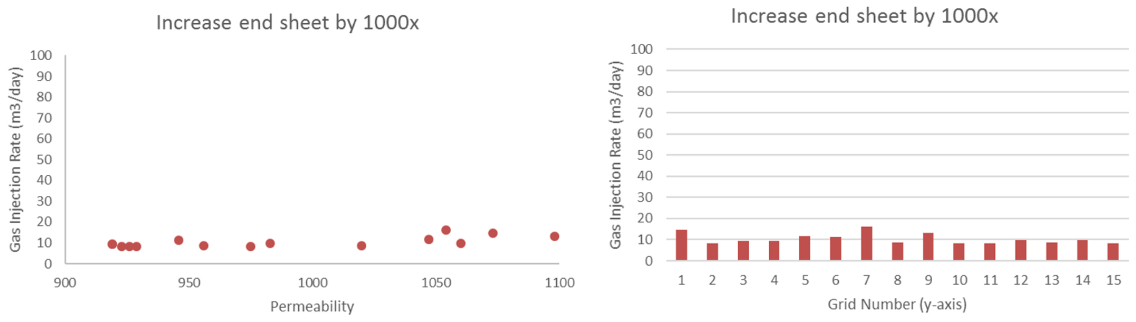

Figure 15: Permeability perturbation with increased end sheet permeability. Left: Correlation between gas injection rate and permeability. Right: Gas injection rate profile.

Reduce permeability in ZY plane of the production-well side

We would also like to check if the absence of an open boundary would lead to an increase in non-uniformity of gas injection. Ideally, a reduction in permeability at the end sheet relative to the rest of the reservoir values should give the opposite effect. In this case, end sheet permeability is reduced by a factor of 10 from the base case. The result is an increased pressure gradient, intensifying the flow towards one grid block, as seen in the base case. This is numerically validated by the increase in CV from 1.398to 1.951.

Redistribute permeability perturbations

We believe that the tendency of gas-injection rate to be high at the heel of the well is because of the current permeability distribution. Although the perturbation was randomized, coincidentally, the second-highest permeability is located at the heel, i.e. 1st grid block. To test this hypothesis, we swap the high-permeability grid blocks toward to the left of the production well with the low-permeability grid blocks on the right side. Specifically, we substituted the following permeability values: 1st and 15th, and 5th and 14th, grid blocks. Now, all the high-permeability grid blocks are situated toward on the right side, while the low-permeability grid blocks are on the left (see **Figure 16**).

Results of the simulation show that there is change in the gas-injection profile. The highest injection rate is still on the first grid block but is now reduced from 61 Sm^3/day in the base case to 42 Sm^3/day. In spite of the change in injection rate, the CV remains high, at 0.962, which suggests that permeability distribution (at least with the modest perturbations here) does not have a significant impact on the location of the highest gas injection rate. This outcome suggests that there are other stronger factors that influence uniformity of injection, such as well placement, as demonstrated by the previous cases.

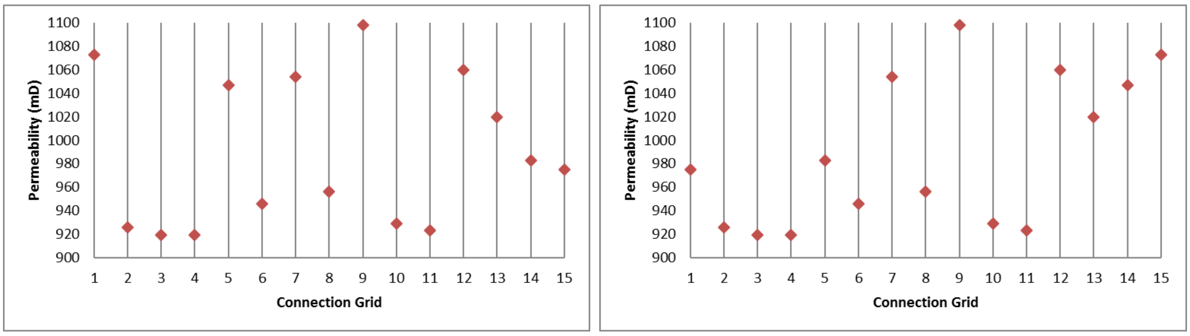

Figure 16: Redistribution of permeability perturbation. Left: Base case. Right: and redistributed.

3.1.5 Effect of changes in fluid properties

Gas viscosity

Ranjan (2015) studied the effects of varying the gas viscosity on the gas-injection profile. He found that doubling gas viscosity increases non-uniformity of injection, while halving gas viscosity decreases non-uniformity. Since viscosity is inversely related to mobility, the results from that study did not meet our expectation. We speculate that not only mobility is the decisive factor, but also mobility ratio. The magnitude of gas viscosity after it has been doubled is still significantly smaller than water viscosity, and thus leads to a small change in the ratio. Therefore, we ran additional simulations with higher gas viscosity values.

Gas viscosity equal to water viscosity

Figure 17 shows the results when gas viscosity is set equal to 1.0144 cP, approximately equal to water viscosity. Unlike the case of Ranjan, where the gas viscosity is doubled, the injection profile is more uniform, though in both cases viscosity is increased. Numerically, the increase in non-uniformity is quantified by a CV of 0.035, which is significantly lower than the non-uniform base case. Moreover, there is a stronger correlation between gas injection rate and permeability as shown in **Figure 18**. The result is as expected, because of the lower gas mobility when its viscosity is increased. The lower mobility prevents the gas from moving freely to its neighbors and it also reduces the mobility ratio, which is associated with flow instabilities.

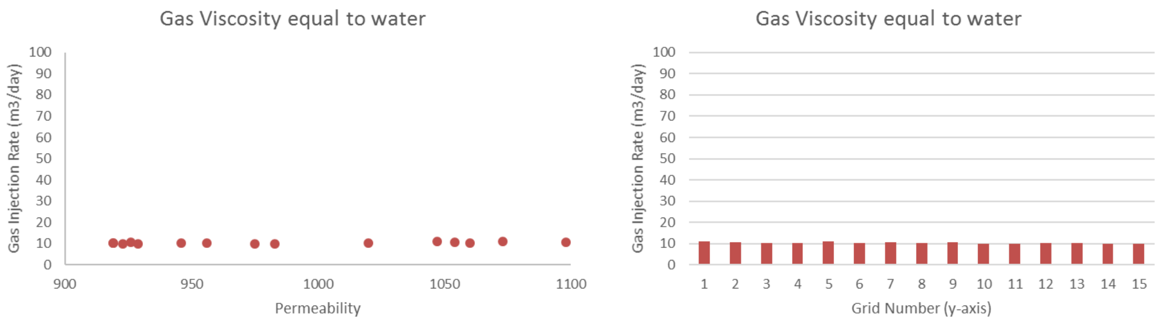

Figure 17: Permeability perturbation, with gas viscosity equal to water. Left: Correlation between gas injection rate and permeability. Right: Gas injection-rate profile.

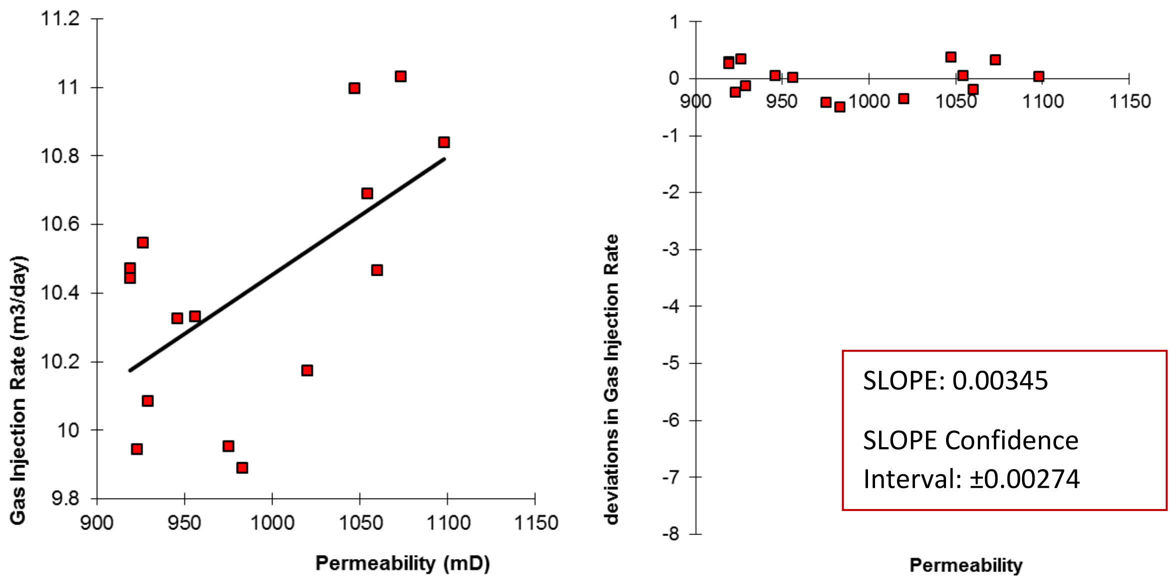

Figure 18: Correlation between gas-injection rate and permeability with 95% confidence interval

Relative permeability

Ranjan (2015) also looked into the effect of variation of Corey exponents for relative permeability This variable controls how sensitive the relative permeability is to changes in the saturations. The value used in the base case of the study for water and gas are 2 and 2.5. Since they are similar, the relative permeability curves are similar. Results from Ranjan (2015) show that a lower Corey exponent leads to a more-uniform injection profile, and a higher saturation exponent leads to more non-uniformity. **Figure 19** shows the effect of changes in the gas saturation exponent.

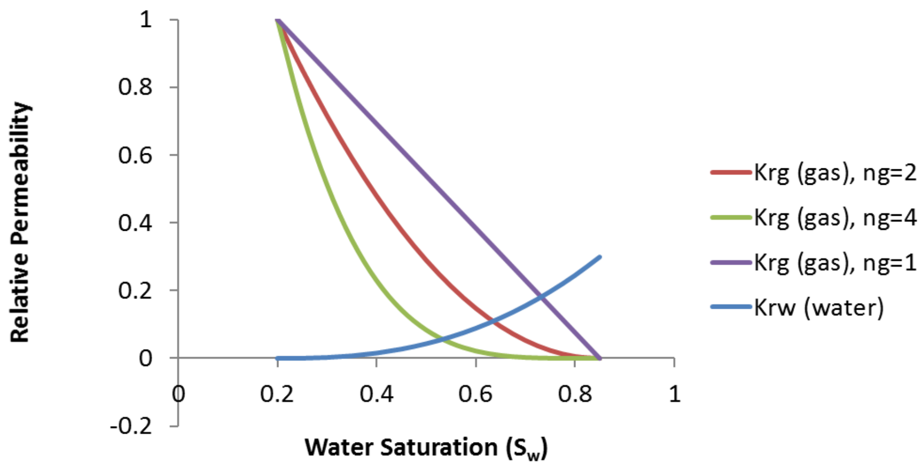

Figure 19: Variation of gas relative-permeability curve in response to changes in gas saturation exponent

We believe that the difference in relative permeability curves may have an impact on non-uniformity of gas injection. The intersection of relative permeability curves is on the right side of the mid-point saturation, meaning that the reservoir is water wet. Therefore, we followed up by running simulations with swapped relative-permeability function parameters of gas and water, to reduce the wettability to water.

Gas relative permeability function parameters swapped with water

Unfortunately, Eclipse does not allow equal relative permeability functions. If water relative permeability is monotonically increasing, then gas relative permeability must be monotonically decreasing. Since we cannot make the functions equal, we swapped the parameters of the functions instead. The effect of the changes to the relative permeability is shown in **Figure 20**.

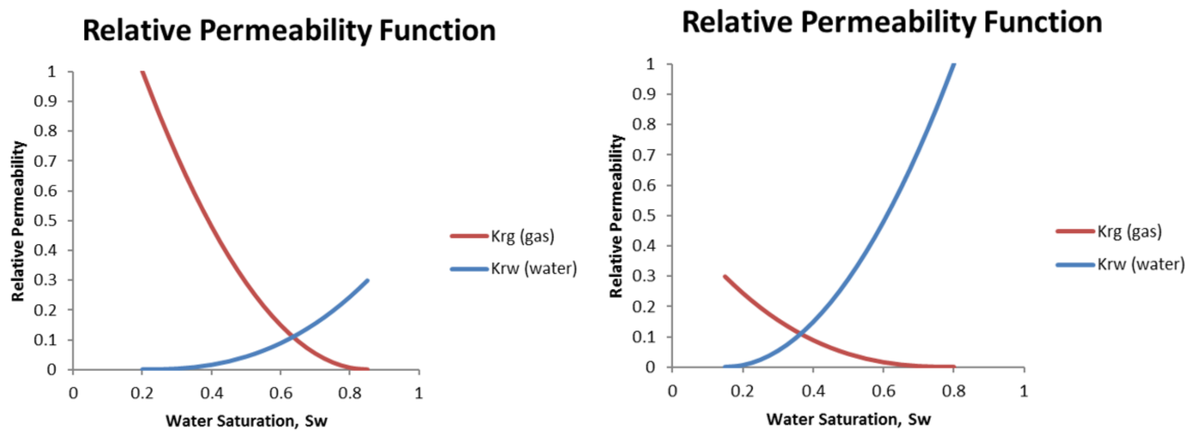

Figure 20: Relative permeability function of base case (left), and swapped parameters (right).

Figure 21 shows the results when relative-permeability function parameters are swapped. This includes swapped parameters such as end-point relative permeabilities, residual saturations and saturation exponents. Like the change in viscosity, there is a significant decrease in CV from 1.398 in base case to 0.143.

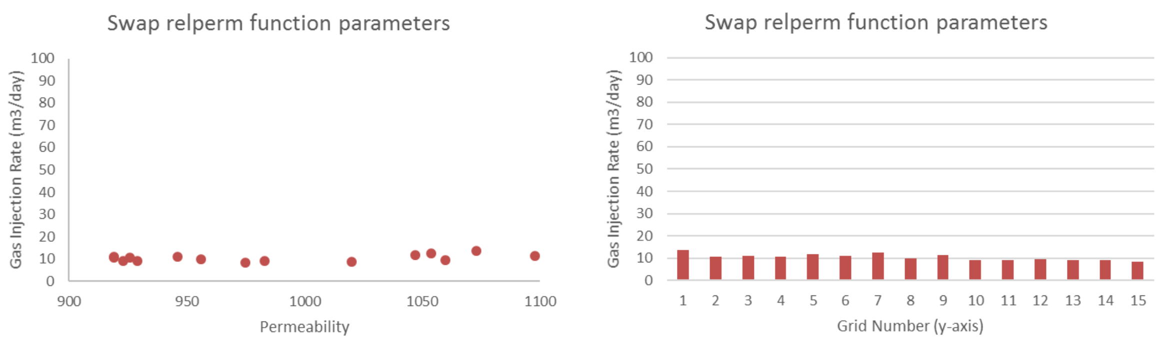

Figure 21: Permeability perturbation with gas and water relative-permeability function parameters swapped. Left: Correlation between gas injection rate and permeability. Right: Gas injection-rate profile.

Viscosity and relative permeability directly affect mobility of each fluid phase, and ultimately the mobility ratio. The latter is used to evaluate whether viscous fingering is occurring in multiphase flow in porous media. We suspect that the non-uniformity of gas injection is due to viscous fingering. In a dipping reservoir, the onset of fingering not only depends on the variations in viscosity but also the velocity of displacing fluid. The higher the velocity, the higher the likelihood of fingering. The maximum velocity that the displacing fluid can flow before the instability develops is referred to as the critical velocity. Therefore, we have run further tests by changing injection rates, as described in the next section.

3.1.6 Effect of changes in operating constraints

Ranjan (2015) studied the effect of changes in gas injection rate to validate results obtained by Jamshidnezhad (2010). However, results were contradictory. While Ranjan (2015) observed an increase in non-uniformity when gas injection rate is doubled, Jamshidnezhad (2010) obtained the opposite. Similarly, different results were also found when gas-injection rate is halved. Instead of increasing only gas injection rate, as Jamshidnezhad (2010) did, we have decided to increase the total injection rate, such that the same injected fluid composition is maintained with 29% water flow rate.

Halve total injection rate

Figure 22 shows the effect of halving the total injection rate. When the total injection rate is reduced from 220 to 110 m^3/day, the gas injection profile becomes more uniform, as indicated by a decrease in CV to 0.208.

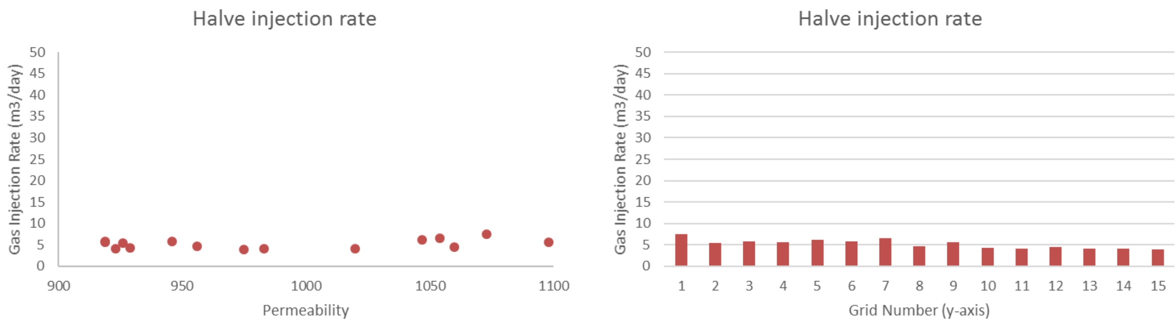

Figure 22: Permeability perturbation with total injection rate halved. Left: Correlation between gas injection rate and permeability. Right: Gas injection-rate profile.

Double total injection rate

Figure 23 shows that effect of doubling total injection rate. We can observe the opposite effect compared to the previous case, i.e. the gas-injection profile becomes more non-uniform in this case. This is numerically indicated by the increase in CV to 2.294.

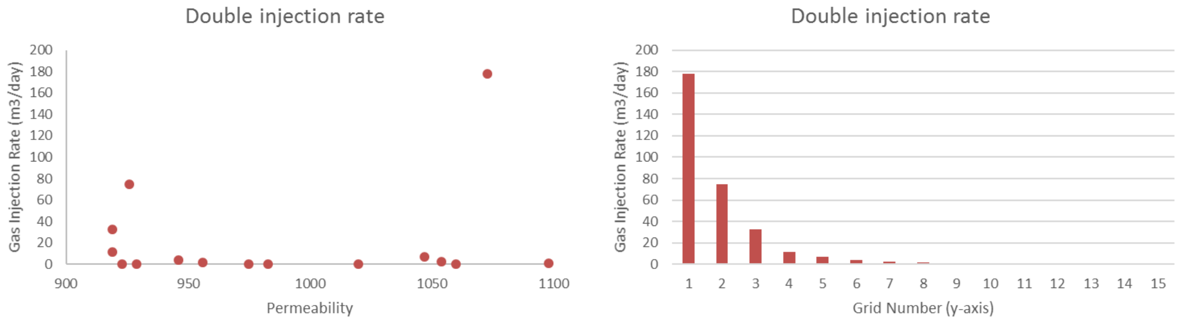

Figure 23: Permeability perturbation with total injection rate doubled. Left: Correlation between gas injection rate and permeability. Right: Gas injection rate profile.

Initially we speculated that the change in injection rate would result only in a difference in the time taken to develop non-uniformity. For this reason, we had expected that when the injection rate is halved, the simulation time required to reach the same level of injected pore volume and, thus non-uniformity would be doubled. However, further simulations run with extended simulation times do not result to significant changes in non-uniformity, at the same injected pore volume or even greater injected pore volume compared to the base case.

3.2 Cases with perturbed skin factor

Based on the study by Van der Bol (2007), it was found that non-uniformity develops even in a completely homogenous reservoir. However, it took a much longer simulation time to develop. Therefore, small permeability perturbations along the injection wells were then introduced to accelerate the occurrence. Subsequent studies then followed the same method by applying ±10% perturbations. What has not been considered is the possibility that this difference in permeability also affects flow to neighboring grid blocks in the y-direction and x-direction, not only injectivity into the grid block. Previous studies show that reducing the y-direction permeability to zero in the injection-well grid blocks, makes the gas-injection profile becomes more uniform. This is because flow is governed by the transmissibility, which is a function of permeability of two adjacent grid blocks and its geometry.

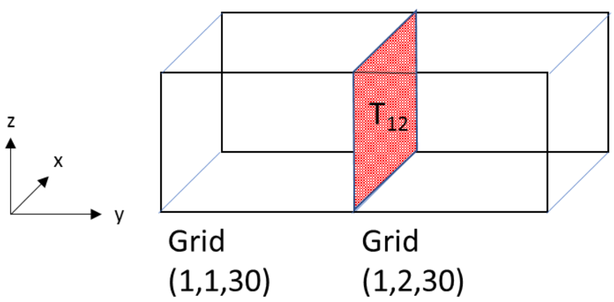

$$T_{12} = \left(\frac{1}{T_1} + \frac{1}{T_2}\right)^{-1}$$

$$T_1 = \left(\frac{K_1 A}{\frac{dy}{2}}\right), T_2 = \left(\frac{K_2 A}{\frac{dy}{2}}\right)$$

Figure 24: Transmissibility between two grid blocks

An alternative method to introduce perturbation without affecting transmissibility and flow to neighboring grid blocks is to vary the skin. This parameter only affects the near-wellbore region, and thus only affects the flow from the well node to the grid block containing the well. The transmissibility between grid blocks remain constant because permeability is unchanged.

Comparison of results with permeability perturbation

Figure 25 shows the comparison between the base case of different perturbation methods. With both perturbations methods, the same injectivity indices were set in the model. The skin was calculated based on a permeability of 1000 mD, and an injectivity index value taken from the permeability perturbation case. Results show that the injection profile becomes more non-uniform by changing from permeability perturbations to skin perturbations, as indicated by the increase in maximum injection rate and an increase in CV from 1.398 to 2.307.

Figure 26 shows the comparison for the case where production well is positioned in the middle, which is on the 8th grid block in y-direction. Unlike the base case, there is a significant difference in gas injection profile. Not only has the injection become qualitatively non-uniform, but also the position of maximum injection rate has shifted to the grid block with the lowest skin.

Parameters that lead to the decrease of CV in one type of perturbation also lead to the decrease in the other. The difference between the results from each method of perturbation is the number of simulation cases that are qualitatively uniform. We can see from **Figure 27** that there are seven relatively uniform simulation cases with the permeability perturbation, while there are only three with the skin perturbation. The three parameters are injection rate, viscosity and relative-permeability function. In both methods of perturbation, these three parameters consistently result in a relatively uniform injection profile, as indicated by the substantial decrease in CV.

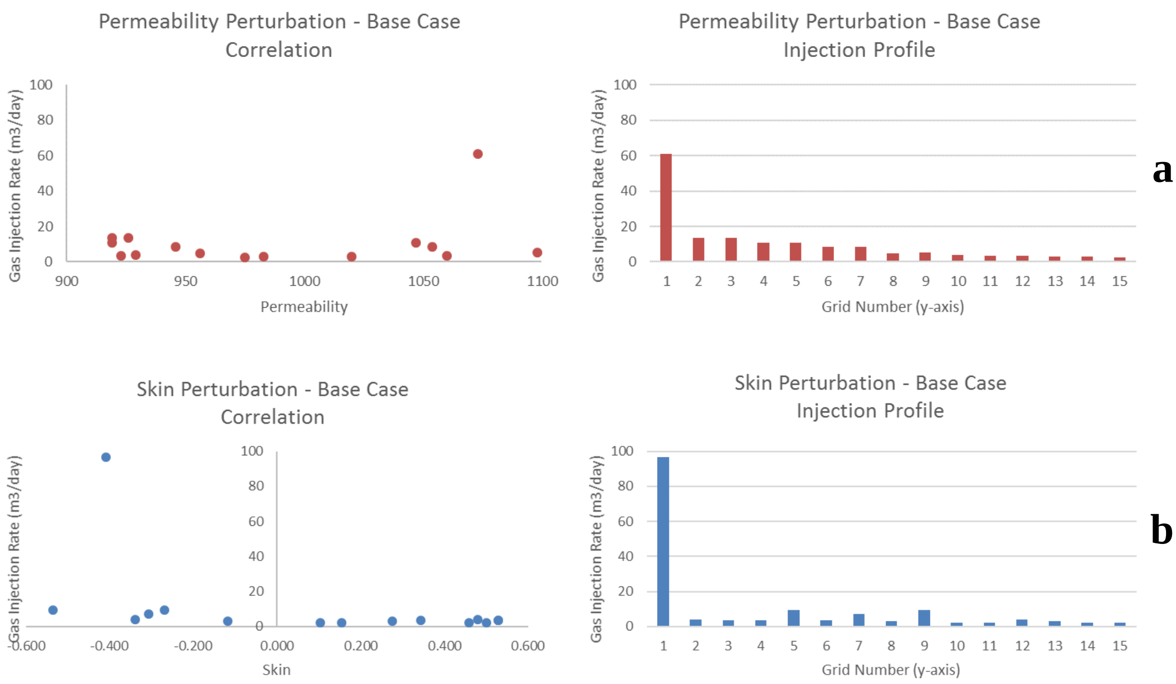

Figure 25: Comparison between the base case of permeability perturbation (a) and skin perturbation (b).

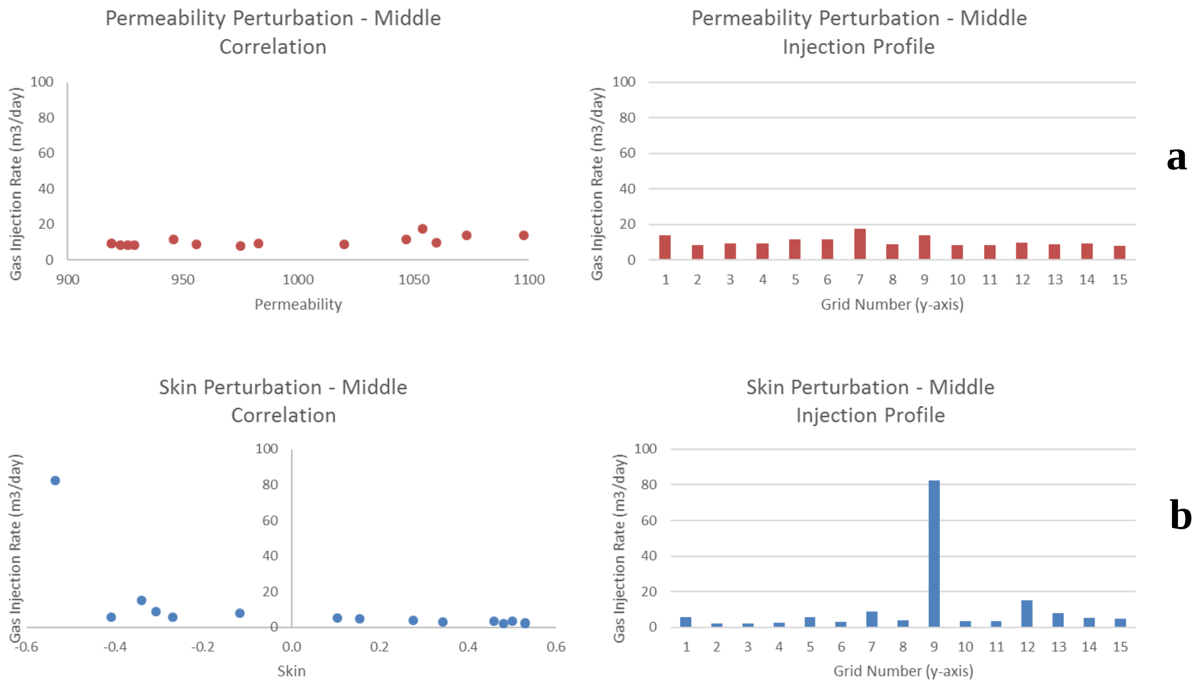

Figure 26: Comparison between permeability perturbation (a) and skin perturbation (b) for the case of production well in the middle, at the 8th grid block in y-direction.

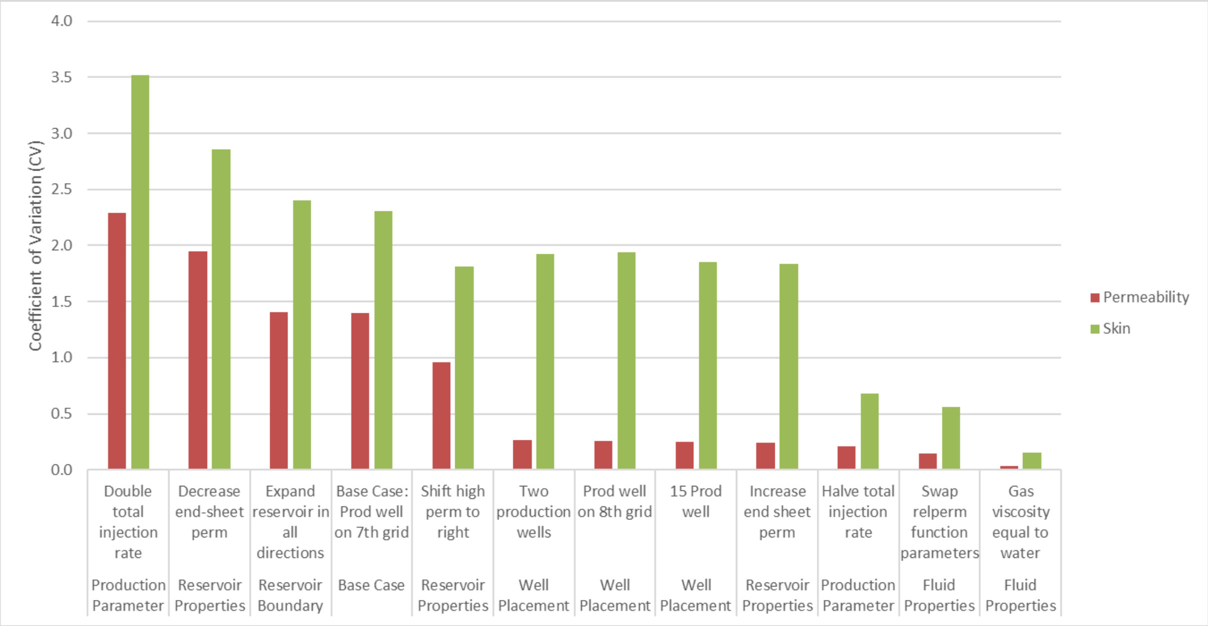

Figure 27: Comparison of CV between permeability and skin perturbation.

3.3 Comparison of a simplified analytical model and simulation

The analytical model described in this thesis is based on a simplified equilibrium between two grid blocks: the gas injection well grid block and the adjacent grid block directly downstream in the x-direction. Although it is believed that neighboring grid blocks affect non-uniformity, other neighboring grid blocks are excluded from the analysis; see **Figure 28**.

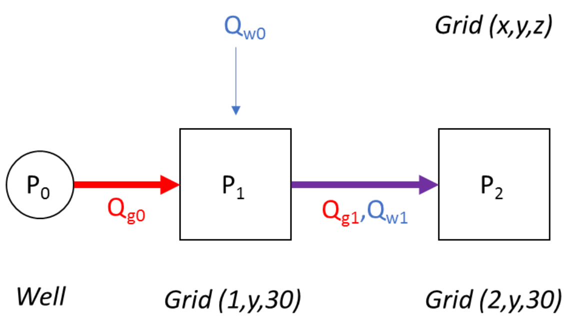

Figure 28: Simplified analytical model

This model is intended to test the hypothesis of Jamshidnezhad (2010) that non-uniform injection results from the feedback between gas-injection rate, water saturation in the gas-injection-well grid block and gas relative permeability.

Equation I describes the flow of gas from the well into the well grid block based on the pressure difference between the bottom-hole flowing pressure in the well (P_0) and the well grid-block pressure (P_1). Equation II describes the flow of gas from the well grid block to the adjacent grid block in the x-direction based on the well-grid-block pressure P_1 and adjacent-grid-block pressure P_2. Q_{w0} is assumed to be fixed in this model. Equation III describes the flow of water to the adjacent grid block. Equation IV is the total flow balance of the well grid block. Equation V describes the change in water saturation based on the difference in water flow in and out of the well grid block.

Simulations were run to determine output parameters used to calculate the constants (C1, C2, C3), see equations I, II, III, V. Due to variation in permeability, the constants vary from one grid-block to another. Therefore, the average value from all 15 grid blocks along the injection well is used for further analysis. Once the constants have been established, the analytical P1 value can be calculated with Equation I. Equations II, III and IV are subsequently used to determine P2. Finally, P2 is plugged into equation III to obtain Q_{w1}, and thus solve for dS_w/dt with equation V. The algorithm is repeated for many values of S_w to create a plot of dS_w/dt vs S_w. A stable condition characterized by little to no change of water saturation over time for a given water saturation. The plot is used together with saturation values from the simulation.

$$Q_{g0} = \frac{C_1(P_0 - P_1)Kk_{rg}\{S_w\}}{\mu_g} \qquad \text{Equation I}$$

$$Q_{g1} = \frac{C_{2g}(P_1 - P_2)Kk_{rg}\{S_w\}}{\mu_g} \qquad \text{Equation II}$$

$$Q_{w1} = \frac{C_{2w}(P_1 - P_2)Kk_{rw}\{S_w\}}{\mu_w} \qquad \text{Equation III}$$

$$Q_{g0} + Q_{w0} = Q_{g1} + Q_{w1} \qquad \text{Equation IV}$$

$$\frac{dS_w}{dt} = C_3(Q_{w0} - Q_{w1}) \qquad \text{Equation V}$$

$$\frac{dS_w}{dt} = \frac{(Q_{w0} - Q_{w1})}{LWH\varphi} \rightarrow C_3 = \frac{1}{LWH\varphi}$$

For the base case, at steady-state condition, water saturation along grid are obtained. Results show that the saturation lie between 0.665 to 0.822. Looking at **Figure 29**, it can be observed that the range of saturation from the simulation lie within the region of instability, where there is some change in saturation over time, and dS_w/dt crosses zero at approximately $S_w = 0.4$.

As a comparison, the same algorithm is run for the case where gas viscosity is increased to a value of equal magnitude to water viscosity. At steady state, results show that the water saturation is between 0.311 to 0.321. **Figure 30**, the range of saturation is situated within the region of stability, where there is hardly any change in saturation over time.

Grid	Sw
1	0.664817
2	0.767889
3	0.765359
4	0.776396
5	0.776408
6	0.783415
7	0.782266
8	0.798591
9	0.796203
10	0.808722
11	0.812265
12	0.814
13	0.818384
14	0.818184
15	0.821826

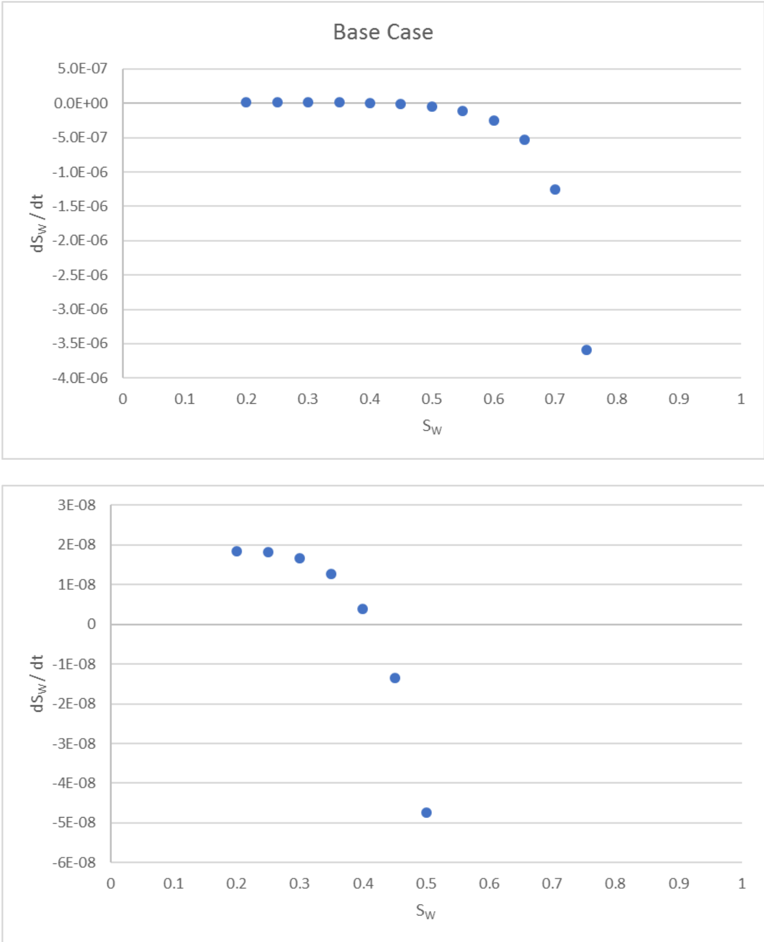

Figure 29: Non-uniform case. Water saturation at steady state condition t = 365 days. Left: simulation results. Right: Analytical plot of dS_w/dt vs S_w. Bottom: Magnified analytical plot between S_w = 0.1 to 0.5

Grid	Sw
1	0.3112094
2	0.3176102
3	0.3162932
4	0.3170431
5	0.3129039
6	0.3164107
7	0.3123034
8	0.3195350
9	0.3130806
10	0.3212594
11	0.3215561
12	0.3172545
13	0.3198997
14	0.3200005
15	0.3218133

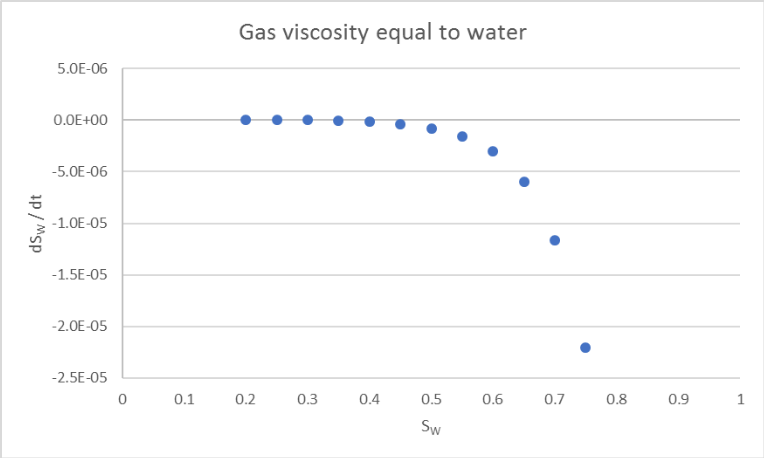

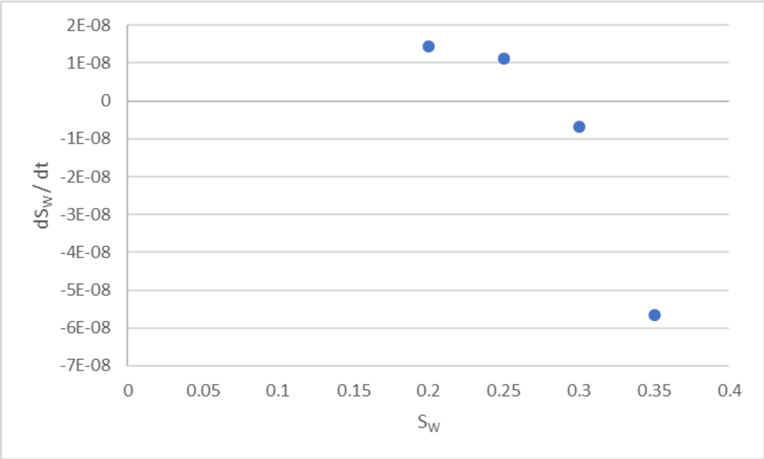

Figure 30: Uniform case. Water saturation at steady state condition at t = 365 days. Left: simulation results. Right: Analytical plot of dS_w/dt vs S_w. Bottom: Magnified analytical plot between S_w = 0.1 to 0.4

Next, we compare the plots of dS_w/dt vs S_w between simulation and analytical results (**Figure 31** and **Figure 32**). Generally, we see a big difference in magnitude from both results, but upon a closer inspection we can see a similar trend (see Appendix **Figure 41** and **Figure 42**). We speculate the big discrepancy in magnitude is caused by simplification of model in our analytical calculations.

Nevertheless, both analytical results from the base case and equal viscosity case show that for a decreasing water saturation, the perturbation would tend to die out. This is not completely true. Based on simulation results, the perturbations diminish only in the equal viscosity case, not in the non-uniform base case. Therefore, the simplified model by itself does not explain the occurrence of instability.

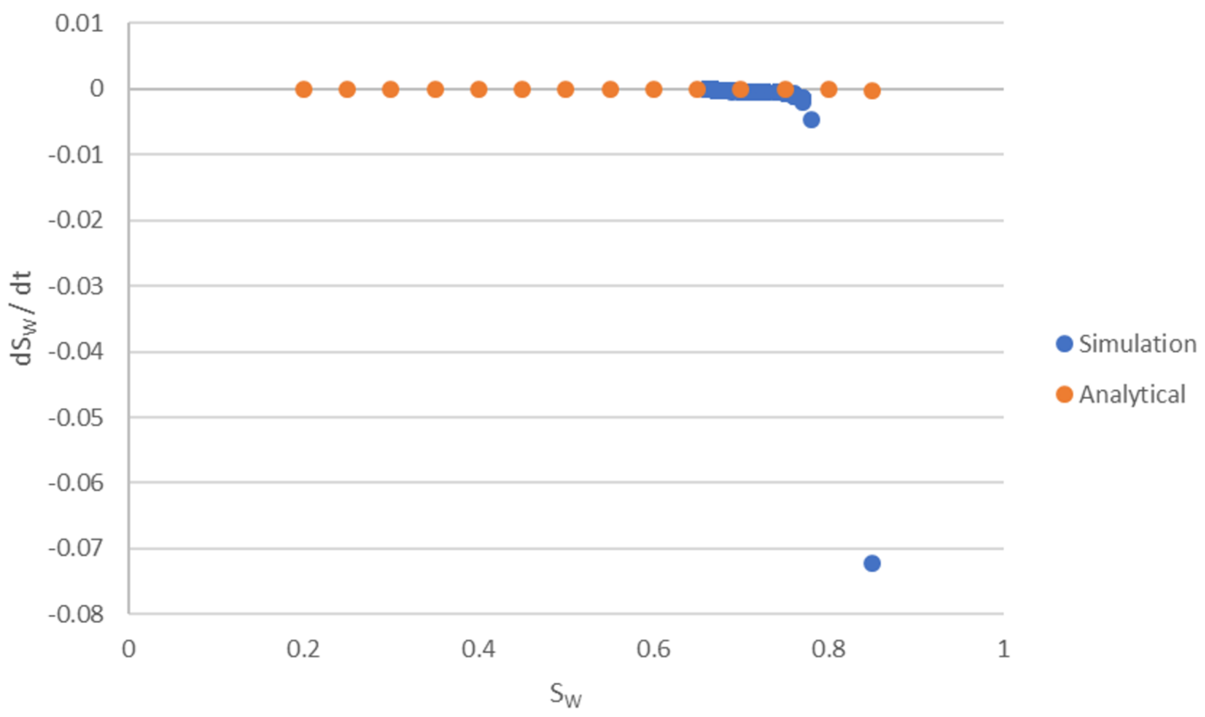

Figure 31: Base case comparison between simulation and simplified analytical model for permeability perturbation

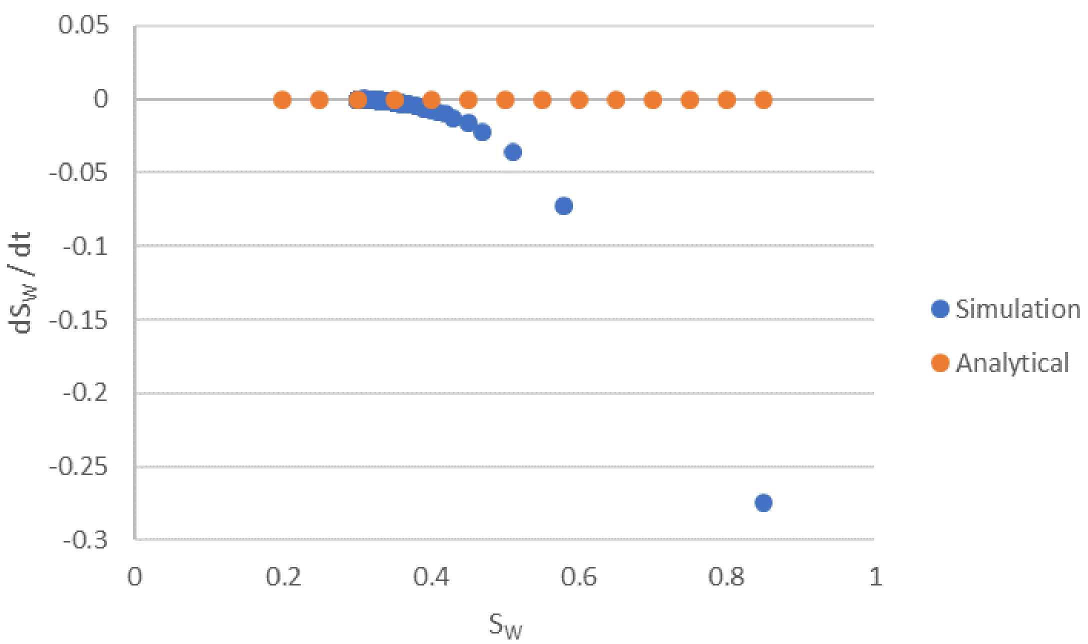

Figure 32: Equal viscosity case comparison between simulation and simplified analytical mode for permeability perturbation

3.4 Effect of mobility ratio on injection profile

The shape of the gas-injection profile along the horizontal well resembles the occurrence of viscous fingering. Gas tends to be issued from one of the grid blocks, bypassing a large section of the reservoir. This creates a non-uniform or fingered profile that is similar to when water is used to drive oil from the reservoir. Viscous flow instability is attributed to high mobility ratio of displacing fluid and displaced fluid. Mobility ratio is a function of relative permeability ratio and viscosity ratio. Therefore, high mobility ratio is caused by high relative permeability ratio and viscosity ratio as shown below:

$$\lambda_g = \frac{kk_{rg}}{\mu_g}\ , \lambda_w = \frac{kk_{rw}}{\mu_w}$$

$$M = \frac{Mobility\ of\ displacing\ fluid}{Mobility\ of\ displaced\ fluid} = \frac{\lambda_g}{\lambda_w} = \frac{k_{rg}}{k_{rw}}\left(\frac{\mu_w}{\mu_g}\right)$$

As an example, in our base case we have taken viscosity of water to be 1 cP and gas viscosity 0.0144 cP at 140 bar. These numbers yield viscosity ratio of approximately 69. Looking at the 1st grid block of gas injection well, at steady state, the relative permeability of gas is 0.0824 and the relative permeability of water is 0.1297, which yields a ratio of approximately 0.6. By multiplying both ratios from the previous calculations, we obtain a mobility ratio of 41. Since M>1 the displacement is unfavorable, where the gas can travel faster than water. This could lead to the non-uniform gas saturation profile.

One way to reduce the mobility ratio is by increasing the viscosity of gas such that it becomes equal or more than the water viscosity. As shown in our simulation, when the gas viscosity is made equal to water viscosity the gas-injection profile becomes more uniform (**Figure 33**). Similarly, when the relative permeability function parameters are swapped, changing the wettability of the formation, more uniform injection is also observed (**Figure 34**). This is valid for both permeability and skin perturbation cases.

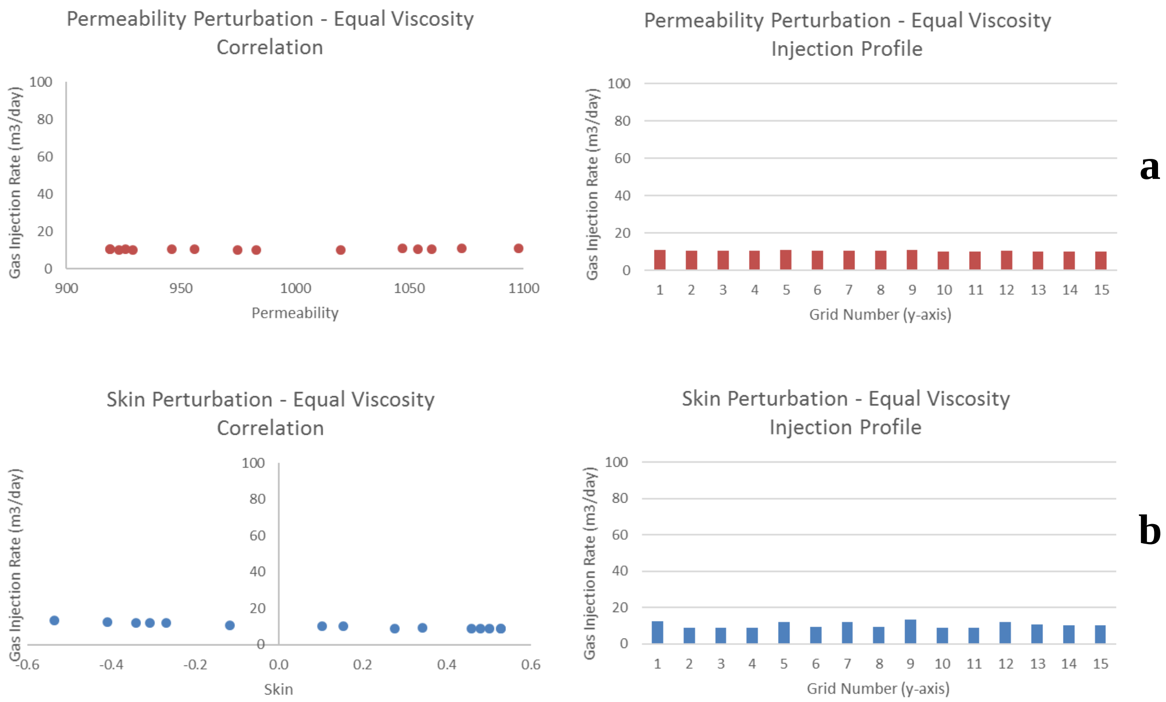

Figure 33: Comparison between a) permeability perturbation and b) skin perturbation for the case of gas viscosity equal to water.

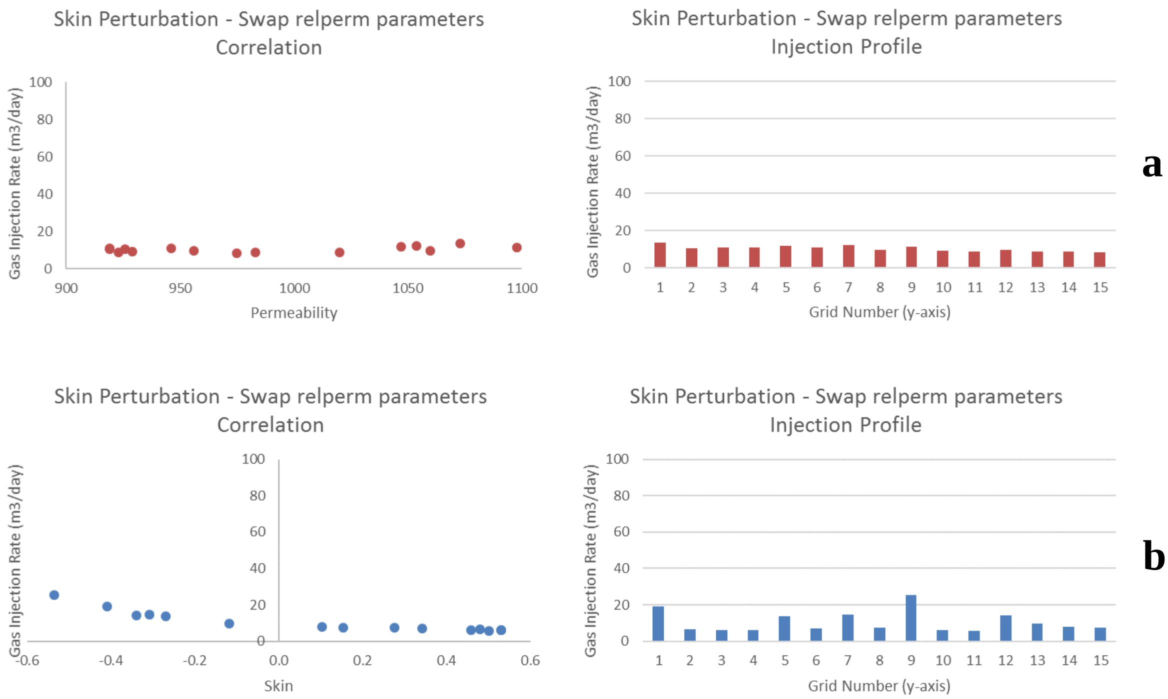

Figure 34: Comparison between a) permeability perturbation and b) skin perturbation for the case of swapped relative permeability function parameters

The question thus arises, if high mobility ratio is the cause of the instability, then for cases with different well placements, the results should all be non-uniform. Parameters than can change the nature of stability would only be viscosity, relative permeability, and injection rate. This is true for the case of skin perturbation. Non-uniform injection is seen even when 15 production wells are placed, simulating flow to an open boundary (**Figure 35**). It is also observed when the production well is placed exactly in the middle of the reservoir, on the 8th grid block in the y-direction of the last grid sheet (**Figure 36**). In those two cases, the location of highest injection rate corresponds to the grid with the lowest skin factor, i.e. the highest injectivity index.

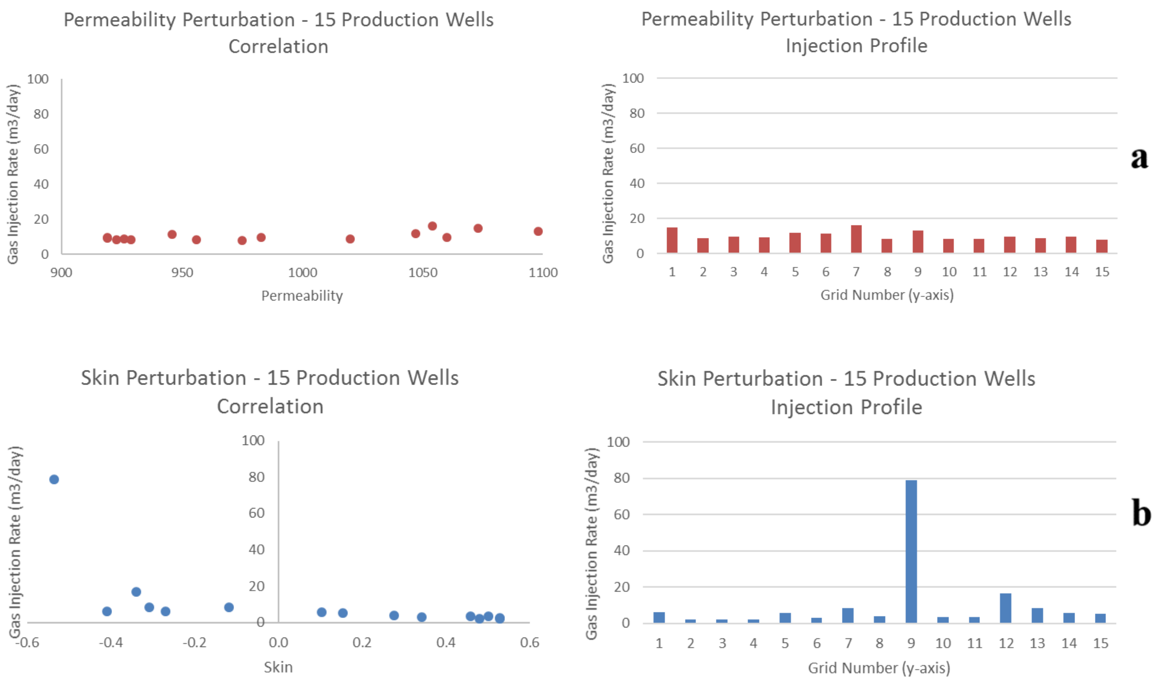

Figure 35: Comparison between a) permeability perturbation and b) skin perturbation for the case of 15 production wells in the last grid sheet.

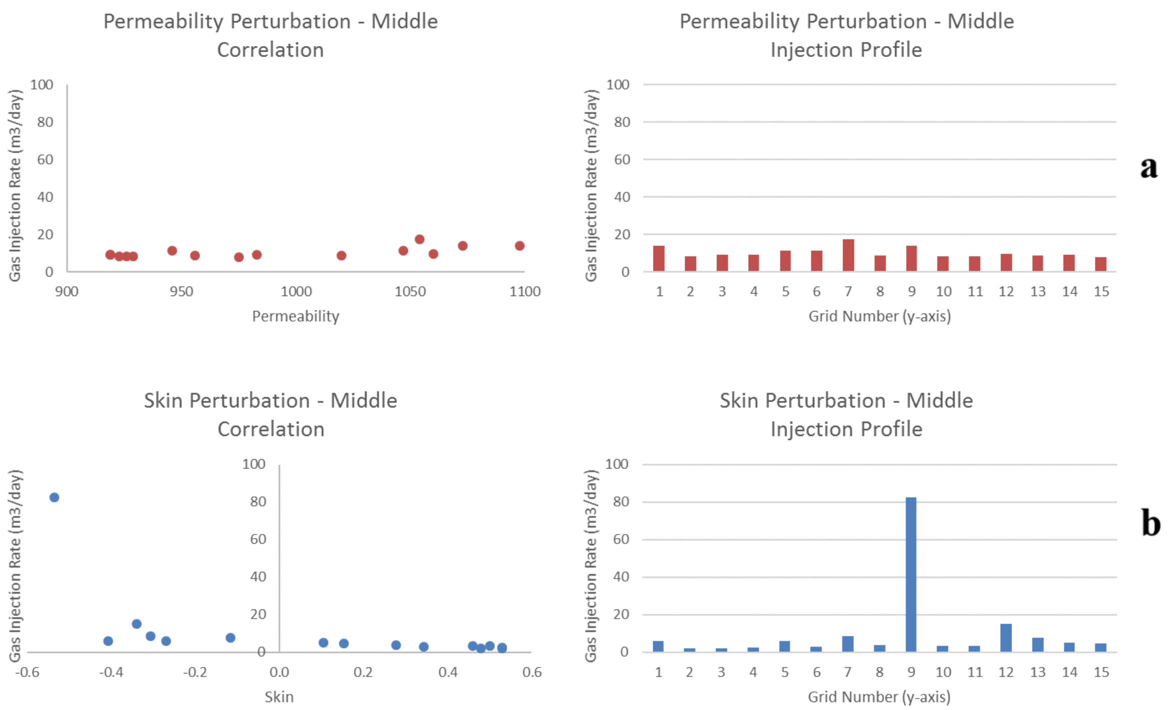

Figure 36: Comparison between a) permeability perturbation and b) skin perturbation for the case production well on the 8th grid block in y-direction of the last grid sheet.

A possible explanation to the uniform injection results in the case of permeability perturbation is the effect of neighboring grid blocks. The difference in absolute permeability between adjacent grids has changed the transmissibility at the interface, which affects the fluid flow. We speculate that the interaction between neighboring grid blocks counters the non-uniformity, that is supposed to develop due to unfavorable mobility ratios.

Figure 37 shows the changes in skin distribution from the base case. The changes made to the skin perturbation is identical to the changes made in permeability perturbation. The skin value of the 1st grid block is swapped with the 15th, and the 5th is swapped with the 14th. These changes were made to have more low skin values on the right side of the production well and more high skin values on the right.

Figure 38 shows the comparison of redistributed perturbation results with the base case. We speculate that the position of the highest injection rate is dependent on the location of the lowest skin and position of the production well, that is why we see that the maximum gas injection is on the 1st grid block, because the location of the lowest skin is on the left of production well and the well is offset to the left of the center of symmetry.

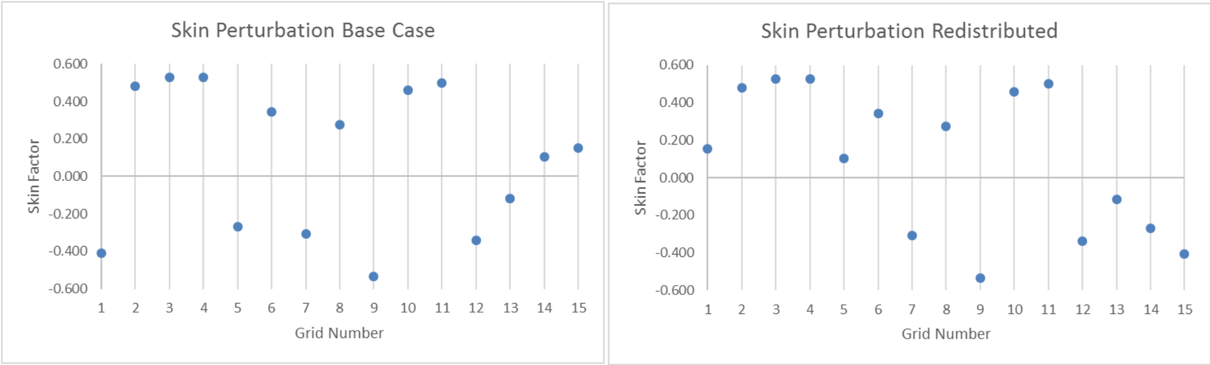

Figure 37: Redistribution of skin perturbation. Left: base case. Right: redistributed case

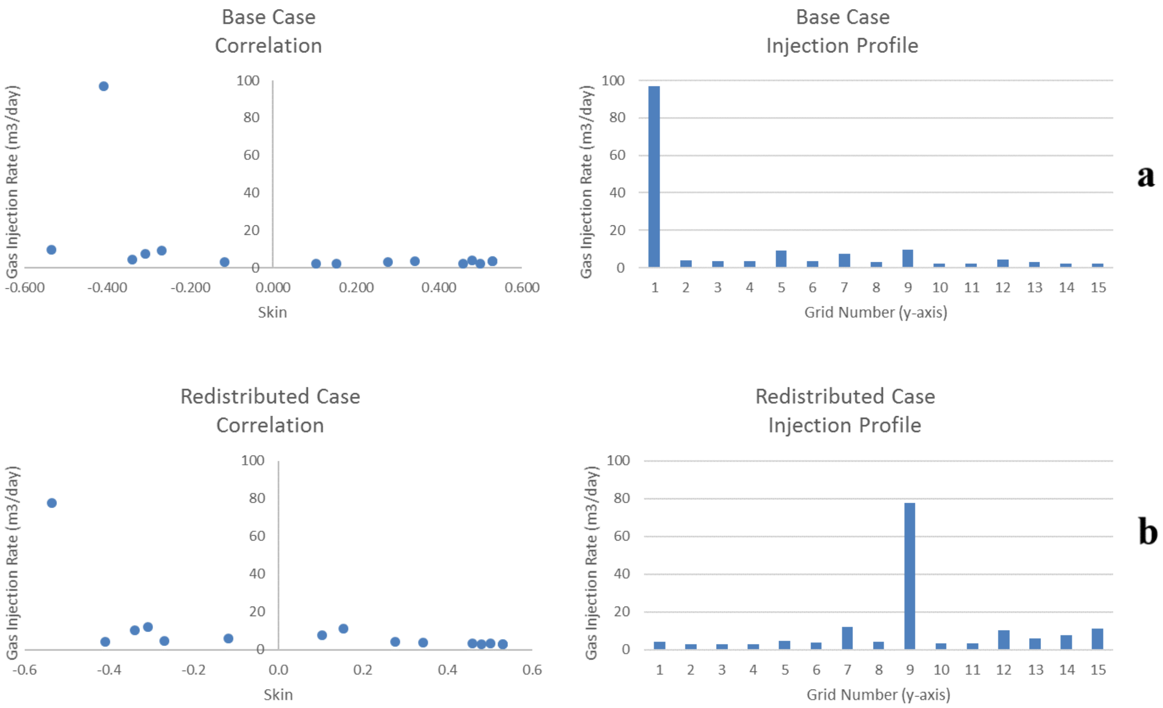

Figure 38: Comparison between a) base case and b) redistributed skin case.

4. Conclusion

From the simulation study, the following conclusions are drawn:

- Non-uniformity can be quantified and compared using the gas-injection rate coefficient of variation and its max-min ratio.
- A possible explanation to the non-uniformity can be that the mobility ratio between displacing fluid (gas) and displaced fluid (water) is high at the gas-injection-well grid blocks, which causes the gas-injection profile to mimic the characteristics of viscous fingering. Water-injection rate remains uniform in all the simulation cases because the mobility ratio is low at the water-injection-well grid blocks. Unlike other parameters, regardless the type of perturbation, results are always consistent in our study when the mobility ratio is modified.

Case of perturbed permeability:

- Production-well placement affects the non-uniformity of gas injection. Depending on the location and number of the production wells, the change can either contribute to increasing or reducing the non-uniformity.
- A better representation of the open boundary leads to a more-uniform gas-injection profile. This can be done either by placing 15 production wells or significantly raising the permeability in the end-sheet grid blocks.
- Together with well placement, distribution of permeability along the injection well plays a role in setting the location of highest injection rate in the non-uniform gas-injection cases.
- We re-examined the effects of gas viscosity found by Ranjan (2015). At viscosities close to water, we observe an increasing uniformity of injection rate when gas viscosity is increased. Meanwhile, at viscosities much lower than water we observe a decreasing uniformity.
- Reservoir wettability affects non-uniformity. This is validated by swapping the relative permeability function parameters for gas and water, such that the curve intersection shifts to the left. This causes the relative permeability, and thus mobility, of gas to decrease, making it more difficult for the gas to flow in the reservoir.
- The effect of increasing either the gas-injection rate only or the total injection rate is the same. Both lead to increasing non-uniformity. Decreasing the rates has the opposite effect. We speculate that reducing injection rate does not slow down the onset non-uniformity, because even at extended simulation times, the uniformity of the gas injection profile is maintained.
- The simplified model describes the feedback between Q_g, S_w, and k_{rg}. However, the model itself does not fully explain the non-uniformity. Adjacent grid blocks need to be considered.

Case of perturbed skin:

- Changes in injection rates, relative permeability functions, and viscosities significantly alter the gas-injection profile, while other parameters do not. We speculate that the effect of neighboring grid blocks is greatly reduced in the case of skin perturbation because the transmissibilities between grid blocks are not affected. We believe that in the case of permeability perturbation, the effect of neighboring grid blocks counters the non-uniformity, such that there is better dispersion of gas-injection rates. For this reason, we see more simulations that depict uniform gas injection in the case of permeability perturbation than in the case of skin perturbation.

5. References

1. Algharaib, M. K., Gharbi, R. B., Malallah, A., & Al-Ghanim, W. (2007, January 1). Parametric Investigations of a Modified SWAG Injection Technique. Society of Petroleum Engineers. doi:10.2118/105071-MS
2. Aziz, K. and Settari, A. (1979). Petroleum Reservoir Simulation. Elsevier Applied Science Publishing Co., Inc., New York.
3. Babu, D. K., Odeh, A. S., Al-Khalifa, A. J., & McCann, R. C. (1991, August 1). The Relation Between Wellblock and Wellbore Pressures in Numerical Simulation of Horizontal Wells. Society of Petroleum Engineers. doi:10.2118/20161-PA
4. Chen, Z., Huan, G., & Ma, Y. (2006). Computational Methods for Multiphase Flows in Porous Media. Philadelphia: Society for Industrial and Applied Mathematics.
5. Dietrich, J. K., & Kuo, S. S. (1996, June 1). Predicting Horizontal Well Productivity. Petroleum Society of Canada. doi:10.2118/96-06-04
6. Hustad, O. S., & Holt, T. (1992, January 1). Gravity Stable Displacement of Oil by Hydrocarbon Gas After Waterflooding. Society of Petroleum Engineers. doi:10.2118/24116-MS
7. Jamshidnezhad, M., van der Bol, L., & Rossen, W. (2010, August 1). Injection of Water Above Gas for Improved Sweep in Gas EOR: Nonuniform Injection and Sweep in 3D. Society of Petroleum Engineers. doi:10.2118/138443-PA
8. Mahalle, N. (2013). Injection of Water Above Gas for Improved Sweep in Gas IOR: Non-Uniform Injection and Sweep. MSc Thesis., Delft University of Technology, Delft, Netherlands.
9. Mai, A., & Kantzas, A. (2009, March 1). Heavy Oil Waterflooding: Effects of Flow Rate and Oil Viscosity. Petroleum Society of Canada. doi:10.2118/09-03-42
10. Mattax, C. C., & Dalton, R. L. (1990, June 1). Reservoir Simulation (includes associated papers 21606 and 21620). Society of Petroleum Engineers. doi:10.2118/20399-PA
11. Muggeridge, A., Cockin, A., Webb, K., Frampton, H., Collins, I., Moulds, T., & Salino, P. (2014). Recovery rates, enhanced oil recovery and technological limits. Philosophical Transactions. Series A, Mathematical, Physical, and Engineering Sciences, 372(2006), 20120320. http://doi.org/10.1098/rsta.2012.0320
12. Panda, M., Nottingham, D., and Lenig, D., 2010. Systematic Surveillance Techniques for a Large Miscible WAG Flood, Proceeding of the SPE Oil and Gas India Conference and Exhibition, 20-22 January.
13. Peaceman, D. W. (1978, June 1). Interpretation of Well-Block Pressures in Numerical Reservoir Simulation (includes associated paper 6988). Society of Petroleum Engineers. doi:10.2118/6893-PA
14. Ranjan, R. (2015). Simultaneous Injection of Water Above Gas for Improved Sweep in Gas EOR: An Analytical and Simulation Study on Non-Uniform Injection and Sweep. MSc Thesis., Delft University of Technology, Delft, Netherlands.

15. Rossen, W. R., & Shen, C. (2007, January 1). Gravity Segregation in Gas-Injection IOR. Society of Petroleum Engineers. doi:10.2118/107262-MS
16. Rossen, W.R. & Van Duijn, C. J. (2004). Gravity Segregation in Steady-State Horizontal Flow in Homogeneous Reservoirs. *Journal of Petroleum Science and Engineering. 43* (1), 99-111. http://dx.doi.org/10.1016/j.petrol.2004.01.004
17. Stone, H. L. (2004, January 1). A Simultaneous Water and Gas Flood Design with Extraordinary Vertical Gas Sweep. Society of Petroleum Engineers. doi:10.2118/91724-MS
18. Van der Bol, L. (2007). Evaluation in Three Dimensions of Injection of Water above Gas for Improved Sweep in Gas IOR. MSc Thesis., Delft University of Technology, Delft, Netherlands.
19. Wan, J., Penmatcha, V. R., Arbabi, S., & Aziz, K. (2000, September 1). Effects of Grid Systems on Predicting Horizontal-Well Productivity (includes associated papers 65961 and 66620). Society of Petroleum Engineers. doi:10.2118/65683-PA

Appendix

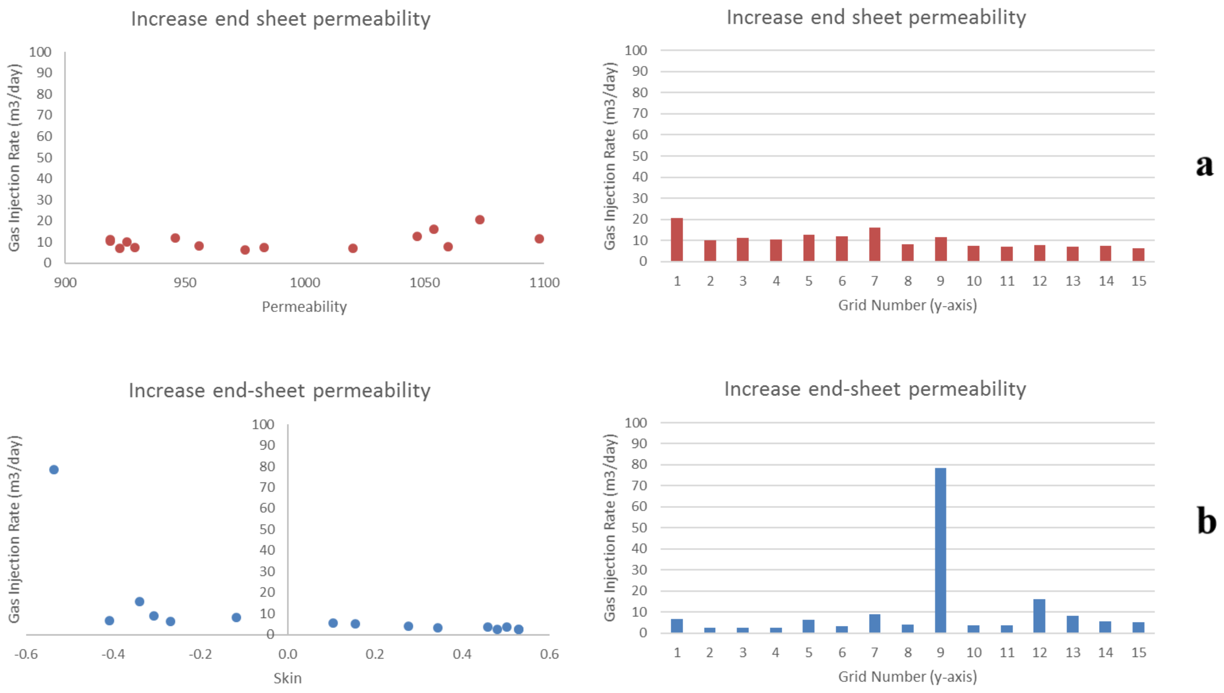

Figure 39: Comparison between a) permeability perturbation and b) skin perturbation for the case of increased end sheet permeability by a factor of 1000.

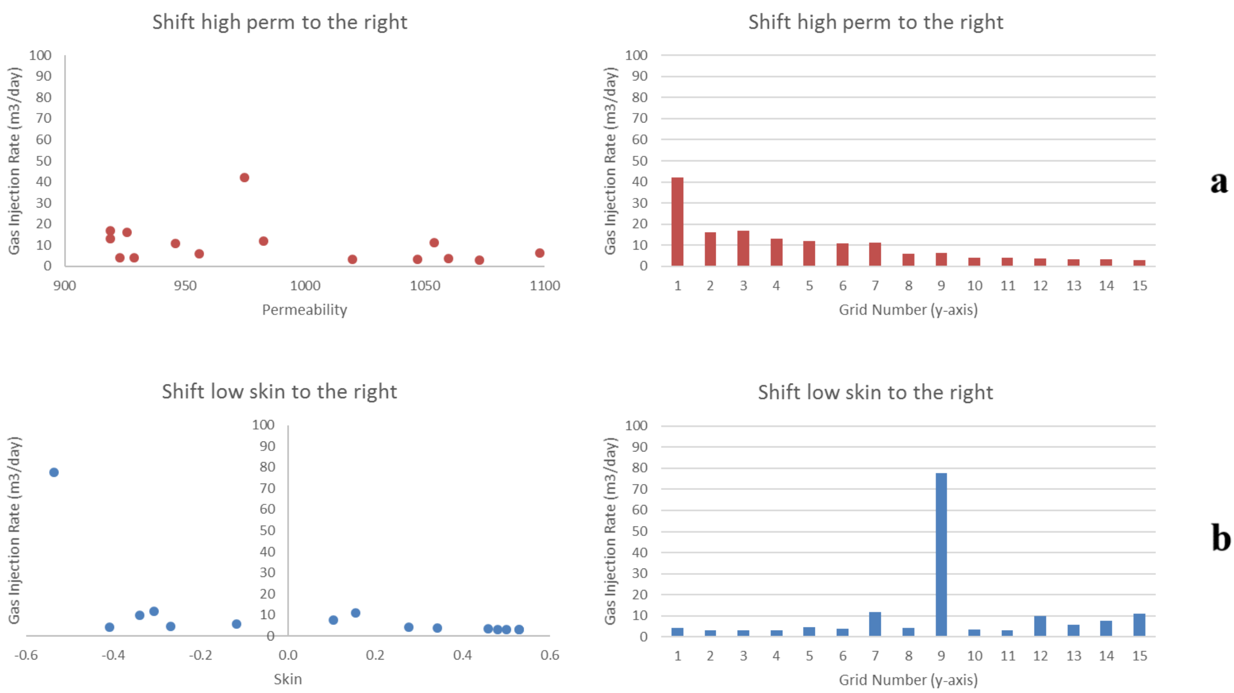

Figure 40: Comparison between a) permeability perturbation and b) skin perturbation for the case of redistributed perturbation.

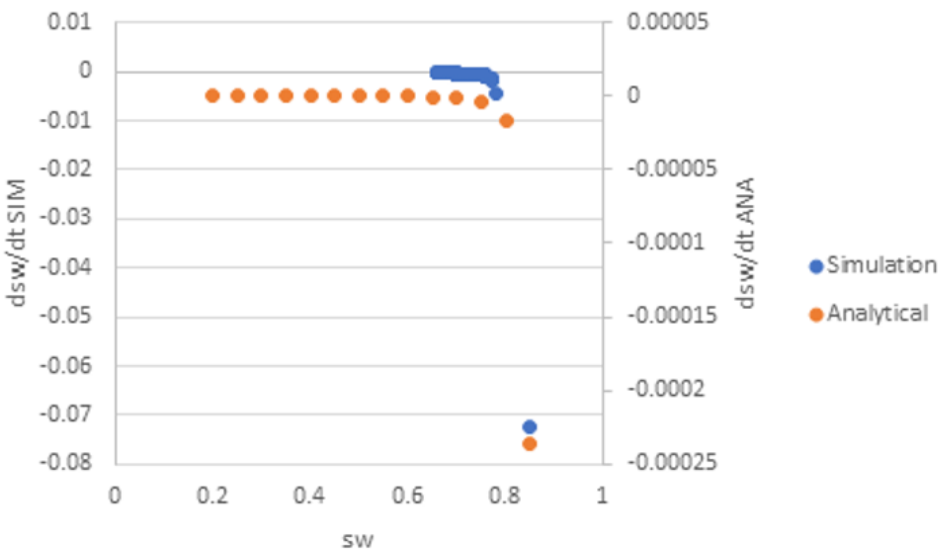

Figure 41: Curve similarity between simulation and analytical results when put on different scales for the Base Case

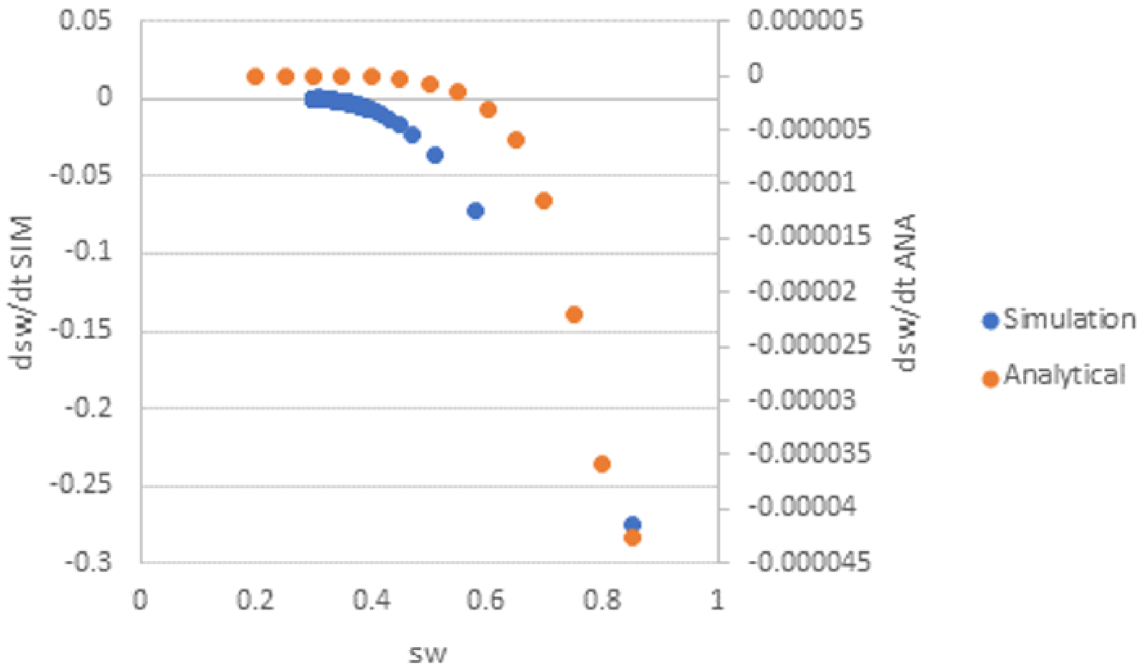

Figure 42: Curve similarity between simulation and analytical results when put on different scales for the equal viscosity case

Table 3: Compilation of simulation results for permeability perturbation

Category	Simulation	Grid Number															STDEV	CV	Max:Min
		1	2	3	4	5	6	7	8	9	10	11	12	13	14	15			
0. Base Case	Base Case	61.097	13.529	13.556	10.693	10.793	8.502	8.653	5.014	5.431	3.791	3.419	3.358	2.961	2.809	2.595	14.556	1.398	23.542
1. Well placement	Production well on th 8th grid block	13.777	8.238	9.354	9.171	11.585	11.540	17.323	8.957	14.013	8.453	8.495	9.608	8.570	9.281	7.836	2.721	0.261	2.211
1. Well placement	15 production wells	15.073	8.622	9.748	9.406	11.681	11.339	16.225	8.582	13.169	8.194	8.353	9.584	8.646	9.508	8.069	2.575	0.247	2.011
1. Well placement	2 Production wells 7th and 9th	14.050	8.356	9.505	9.302	11.718	11.589	17.222	8.913	13.896	8.457	8.512	9.577	8.444	9.050	7.610	2.740	0.263	2.263
2. Reservoir Boundary	Expand all reservoir dimensions	62.392	13.215	10.336	7.436	6.737	5.360	5.426	4.017	4.662	3.962	4.263	5.314	5.968	7.925	9.186	14.613	1.403	15.747
3. Reservoir Properties	Increase end sheet permeability by 1000x	14.794	8.457	9.569	9.310	11.598	11.329	16.327	8.592	13.192	8.185	8.394	9.719	8.806	9.711	8.216	2.544	0.244	1.995
3. Reservoir Properties	Reduce end sheet permeability by 10x	82.181	13.919	13.038	9.616	8.796	6.434	5.812	3.604	3.389	2.302	1.841	1.605	1.328	1.202	1.132	20.312	1.951	72.623
3. Reservoir Properties	Shift high perm to the right	42.133	16.024	16.894	13.212	12.042	10.805	11.138	5.803	6.355	4.247	3.905	3.893	3.395	3.324	3.030	10.020	0.962	13.904
4. Fluid Properties	Gas Viscosity equal to Water	11.032	10.547	10.474	10.445	10.996	10.326	10.690	10.332	10.839	10.086	9.946	10.466	10.175	9.892	9.955	0.367	0.035	1.115
4. Fluid Properties	Swap relperm function parameters	13.564	10.657	11.015	10.749	11.779	11.099	12.454	9.713	11.246	9.099	8.952	9.513	8.933	8.975	8.451	1.486	0.143	1.605
5. Production Parameters	Double injection rate	177.709	75.055	32.344	11.283	6.686	3.702	2.577	1.429	0.962	0.455	0.183	0.016	0.000	0.000	0.000	47.771	2.294	#DIV/0!
5. Production Parameters	Halve injection rate	7.536	5.381	5.752	5.533	6.192	5.747	6.629	4.642	5.678	4.281	4.190	4.444	4.123	4.128	3.844	1.081	0.208	1.961

Table 4: Compilation of simulation results for skin perturbation

Category	Simulation	Grid Number															STDEV	CV	Max:Min
		1	2	3	4	5	6	7	8	9	10	11	12	13	14	15			
0. Base Case	Base Case	96.810	4.006	3.565	3.358	9.231	3.372	7.346	3.012	9.546	2.206	2.022	4.202	3.005	2.332	2.186	24.027	2.307	47.878
1. Well Placement	Production well on the 8th grid block	5.869	2.213	2.203	2.318	5.887	3.107	8.692	3.929	82.318	3.543	3.441	14.962	7.744	5.183	4.791	20.165	1.936	37.367
1. Well Placement	15 production wells	6.120	2.251	2.228	2.331	5.894	3.087	8.536	3.892	78.791	3.519	3.513	16.738	8.473	5.620	5.206	19.276	1.851	35.365
1. Well Placement	2 Production wells 7th and 9th	5.794	2.220	2.204	2.315	5.822	3.100	8.576	3.916	81.628	3.560	3.490	15.497	7.900	5.275	4.903	19.995	1.920	37.043
2. Reservoir Boundary	Expand all reservoir dimensions	100.721	4.195	3.341	2.839	5.495	2.476	4.268	2.272	5.966	2.043	2.106	5.642	4.911	4.550	5.375	25.021	2.403	49.308
3. Reservoir Properties	Increase end sheet permeability by 1000x	6.693	2.393	2.338	2.432	6.207	3.163	8.772	3.909	78.473	3.661	3.490	15.917	8.208	5.428	5.115	19.154	1.839	33.564
3. Reservoir Properties	Reduce end sheet permeability by 10x	117.824	3.969	3.430	3.116	7.050	2.778	4.614	2.112	4.052	1.322	1.104	1.732	1.236	0.963	0.898	29.763	2.858	131.192
3. Reservoir Properties	Shift low skin to the right	4.115	3.059	2.978	3.040	4.695	3.743	11.797	4.161	77.636	3.370	3.127	10.042	5.811	7.612	11.014	18.847	1.810	26.070
4. Fluid Properties	Gas viscosity equal to water	12.566	9.020	9.002	8.917	12.206	9.148	11.999	9.141	13.416	8.866	8.731	12.133	10.864	10.109	10.081	1.633	0.157	1.536
4. Fluid Properties	Swap relperm function parameters	19.166	6.337	6.061	6.009	13.675	6.886	14.658	7.218	25.340	6.096	5.849	14.045	9.856	7.691	7.314	5.829	0.560	4.332
5. Production Parameter	Double injection rate	285.9	8.437	4.241	3.067	4.564	1.741	2.011	0.87	1.027	0.317	0.163	0.09	0	0	0	73.360	3.522	#DIV/0!
5. Production Parameter	Halve injection rate	11.349	2.930	2.794	2.774	7.216	3.163	7.521	3.266	14.230	2.684	2.549	6.674	4.389	3.372	3.189	3.557	0.683	5.583